Supporting Information

Excited-State Lifetimes of DNA-Templated Cyanine Dimer, Trimer, and Tetramer Aggregates: The Role of Exciton Delocalization, Dye Separation, and DNA Heterogeneity

Jonathan S. Huff,[1] Daniel B. Turner,[1] Olga A. Mass,[1] Lance K. Patten,[1] Christopher K. Wilson,[1] Simon Roy,[1] Matthew S. Barclay,[1] Bernard Yurke,[1,2] William B. Knowlton,[1,2] Paul H. Davis,[1] Ryan D. Pensack[1]

[1]Micron School of Materials Science & Engineering and [2]Department of Electrical & Computer Engineering, Boise State University, Boise, Idaho 83706

Table of Contents:

Section S1: Spectrum of white-light continuum probe

For transient absorption experiments, a white light continuum (WLC) probe was generated by focusing a small portion of the regenerative amplifier output onto a sapphire window. Further details are given in the methods section of the main text. **Figure S1.1** below shows a typical spectrum of the WLC probe. A 750 nm short pass filter was used to block residual 800 nm light from the regenerative amplifier.

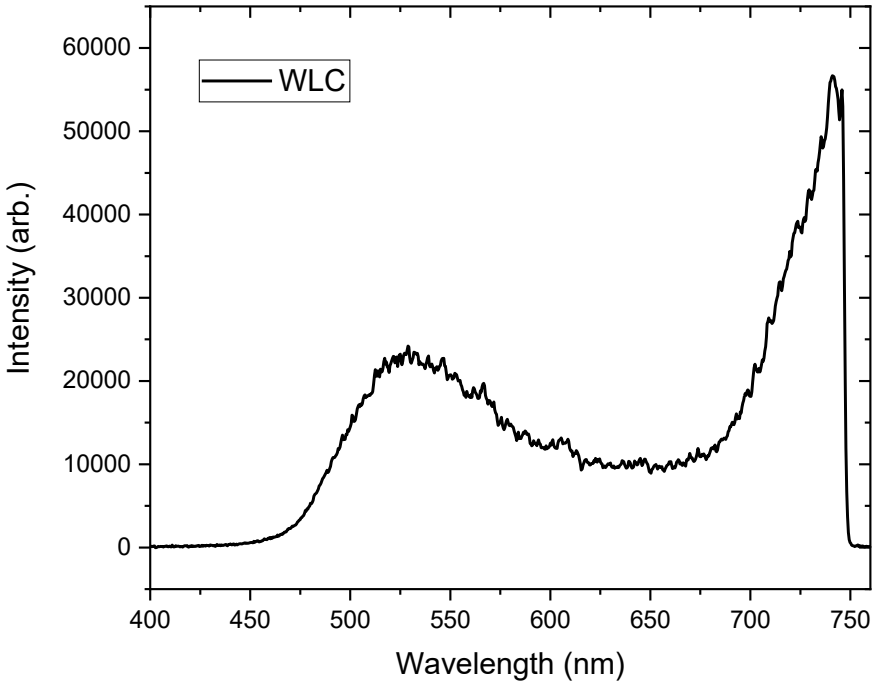

Figure S1.1 Typical white light continuum probe spectrum.

Section S2: Pump pulse autocorrelation indicates sub-200-fs duration

The pump pulse width was measured by performing an autocorrelation of the OPA set to 650 nm. The resulting autocorrelation is plotted in **Figure S2.1**. The full width at half max of the Gaussian fit to the autocorrelation is 180 fs, which represents the duration of the pump pulse at the sample position.

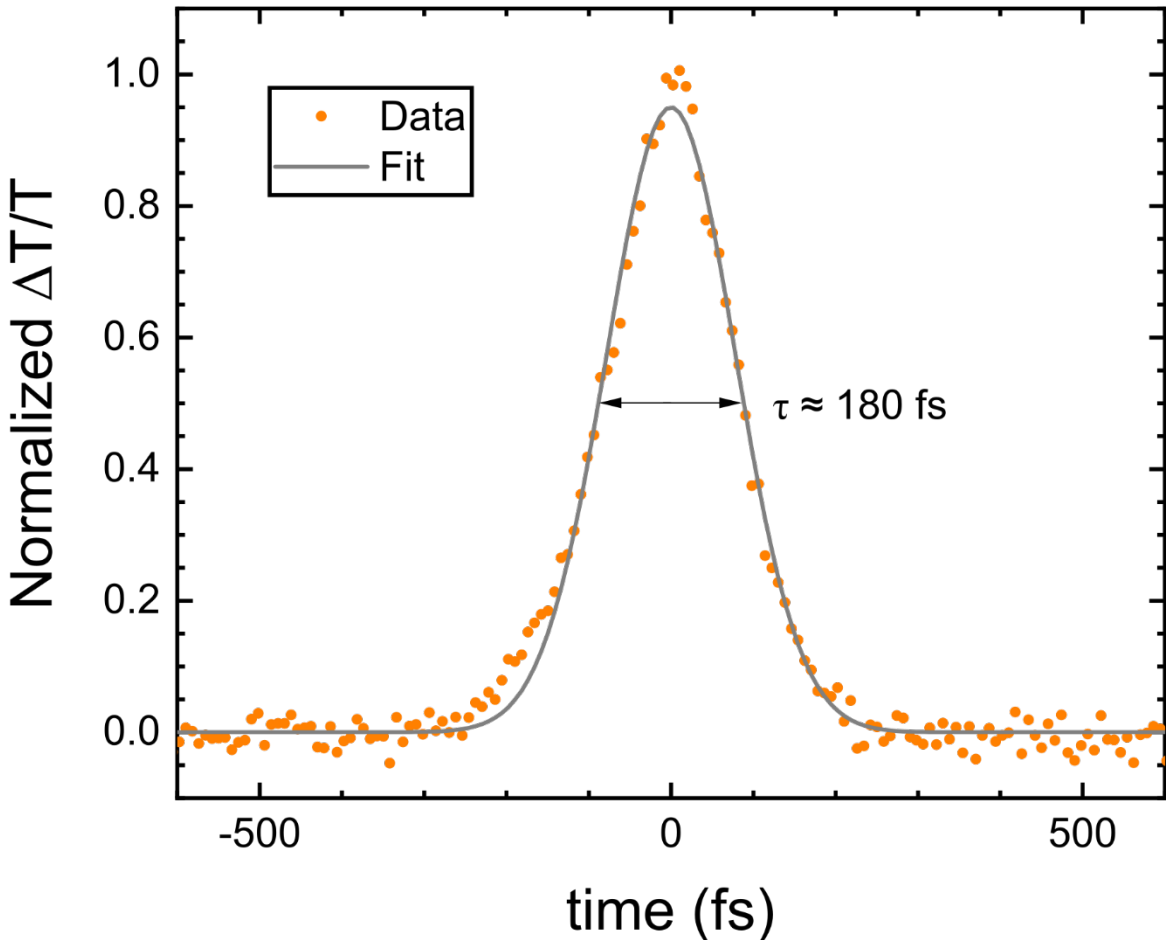

Figure S2.1 Autocorrelation measurement of the duration of the 650 nm pump pulse.

Section S3: Three-component global target analysis of transient absorption of no-salt type 1 solution excited at 675 nm

The transient absorption (TA) collected for the no-salt type 1 (largely duplex dimer) solution excited at 675 nm (and shown in **Figure 2** in the main text) was subject to global target analysis according to the three-component kinetic scheme shown in **Figure S3.1**. In this supporting section, we discuss the physical and mathematical basis for the three components used to model the TA dataset.

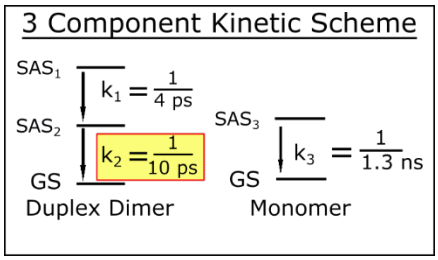

Figure S3.1. The three-component kinetic scheme used in the global target analysis of the transient absorption of the no-salt type 1 aggregate solution excited at 675 nm. Two of the three components in the kinetic scheme account for two subpopulations present in the solution, a large subpopulation of duplex dimer structures and a small subpopulation of monomers. The rate constant associated with the monomer component was fixed to a value of 1/1.3 ns^{-1}, which corresponds to the monomer lifetime of 1.3 ns. A third component is included in the kinetic scheme to account for sequential dynamics of the large subpopulation of duplex dimer structures. Each species associated spectrum, SAS_n, is assigned a rate constant, k_n.

First, we provide physical justification for starting with a two-component kinetic scheme. The physical justification for starting with a two-component kinetic scheme is that the no-salt type 1 solution was previously found to include a small subpopulation of monomers in addition to the duplex dimer structures.[1] Specifically, Huff *et al.* showed that the fluorescence excitation spectrum of the no-salt type 1 solution did not match its absorption spectrum, but rather matched the absorption spectrum of the monomer. These results indicated that a small subpopulation of monomers exists in the solution. Because the current TA measurements were performed with a 675 nm excitation wavelength where the monomer absorbs, we can expect the monomer to contribute to the TA signal. Thus, we start with a two-component kinetic scheme to model the TA dataset.

Next, we provide mathematical justification for including a third component. **Figure S3.2** displays selected kinetics traces and fits returned by performing a global target analysis of the TA dataset according to a two- and three-component kinetic scheme, with the third rate constant associated with the monomer fixed to 1/1.3 ns^{-1} (i.e., corresponding to the monomer lifetime).

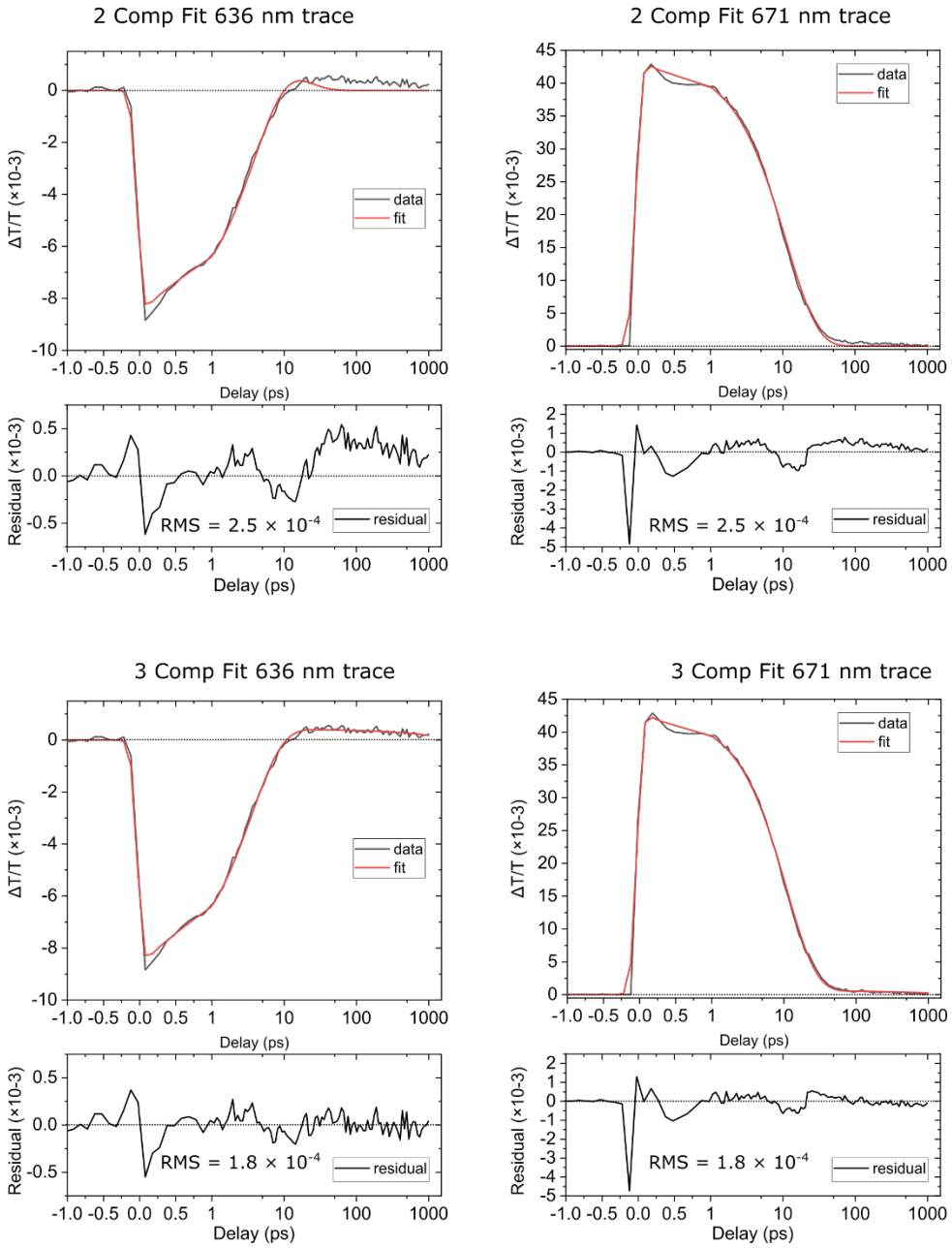

Figure S3.2. Selected kinetics traces (black) and fits (red) taken at 636 and 671 nm, which have been assigned to the excited-state absorption and ground-state bleach and features, respectively, of the duplex dimer structure. (Top left) 636 nm kinetics trace and two-component fit of the data with the fit residual plotted below. (Top right) 671 nm kinetics trace and two-component fit of the data with the fit residual plotted below. (Bottom left) 636 nm kinetics trace and three-component fit of the data with the fit residual plotted below. (Bottom right) 671 nm kinetics trace and three-component fit of the data with the fit residual plotted below.

If we first consider the two-component fit to the 671 nm kinetics trace, which corresponds to the duplex dimer primary ground-state bleach, we see that two components fit the data quite well. This

is consistent with the results reported by Huff *et al*.[1] The two-component fit of the kinetics trace for the excited-state absorption (ESA) at 636 nm, however, clearly is not fit well by two components, as can be seen in the obvious signs of structure in the residual plot at timescales > 1 ps. The addition of a third component greatly improves the fit quality, particularly for the 636 nm kinetics trace for which residual plot shows essentially no structure. Additionally, the 671 nm fit exhibits substantially reduced structure at delays > 50 ps. Also, the RMS value of 1.8×10^{-4} is significantly smaller than the RMS of 2.5×10^{-4} returned from the two-component fit. Though the addition of an additional component may have improved the residual of the 671 nm fit, this was not done due to the lack of a physical basis to include an additional component.

Having determined that three components are needed to model the TA dataset, we next discuss the physical assignment of the third component. As noted above, at least two components, attributable to duplex dimer structures and monomers, are needed to initially model the data. The monomer component, which has the longest lifetime and correspondingly smallest rate constant (i.e., 1/1.3 ns^{-1}), is assigned to SAS_3. Given that previous measurements indicated the excited-state lifetime of the duplex dimer structure is 11 ps and given that the rate constant associated with SAS_2 is 1/10 ps^{-1}, we assign the second component to the duplex dimer structure. Thus, the remaining component to be assigned is associated with SAS_1 with a rate constant of 1/4 ps^{-1}.

To assign the remaining component associated with SAS_1, we need to two consider two scenarios. The two scenarios are: (i) SAS_1 decays sequentially into SAS_2, or (ii) SAS_1 decays in parallel with SAS_2. The first scenario could arise if the duplex dimer structures exhibit complex (i.e., nonmonoexponential) dynamics, and the second scenario could arise if the no-salt type 1 solution exhibited dimer structural heterogeneity. We immediately rule out (ii) based on our previous results indicating the TA of the no-salt type 1 solution is largely invariant to excitation wavelength.[1] Specifically, we showed that the TA kinetics of the no-salt type 1 solution excited and probed at wavelengths of 675 and 600 nm were largely identical, with the exception of an additional minor component appearing in the experiment exciting and probing at 600 nm. These measurements indicated the no-salt type 1 solution is largely homogeneous with respect to aggregates, particularly in the vicinity of ca. 675 nm. Thus, we conclude that the duplex dimer structures exhibit complex (i.e., nonmonoexponential) dynamics, and that SAS_1 decaying sequentially into SAS_2 represents the best description of the TA dataset.

Figure S3.3 displays the SAS derived for the different components according to the three-component kinetic scheme displayed in **Figure S3.1**.

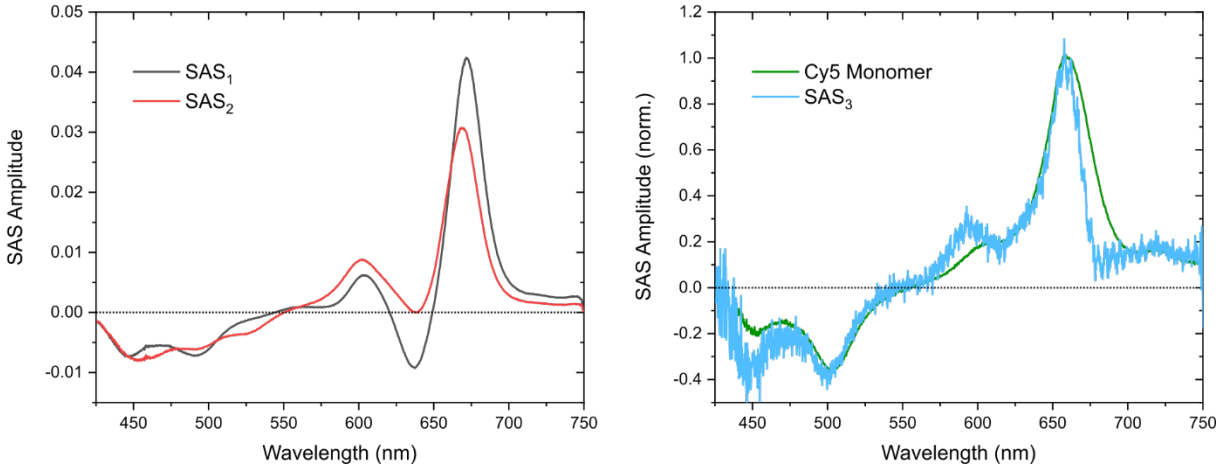

Figure S3.3. Species-associated spectra (SAS) resulting from a global target analysis of the TA of the no-salt type 1 solution excited at 675 nm, with the global target analysis assuming a three-component kinetic scheme. (Left) SAS_1 and SAS_2 are assigned to duplex dimer structures, with SAS_1 decaying into SAS_2. (right) SAS_3 is assigned to a small subpopulation of monomers. SAS_3 has been normalized. Overlaid on the plot for comparison is the normalized monomer transient absorption spectrum.

The left panel of **Figure S3.3** displays SAS_1 and SAS_2 attributed to the duplex dimer structures. Both spectra exhibit overall general agreement with the steady-state absorption spectrum, which is consistent with our assignment of both SAS to the duplex dimer structures. In the case of SAS_1, additional negative amplitude attributable to an (ESA) band is evident at ca. 640 nm. The amplitude of the ESA band has decayed to a large extent in SAS_2. Modeling these data has determined that the rate of this change (k_1) is ~ 1/4 ps^{-1}, which is consistent with the observations reported in **Figure 3** in the main text. We assign SAS_1 to the vertically excited state, and the conversion of SAS_1 into SAS_2 to a dynamic process occurring within the excited state. Critically, the model derives k_2 ~ 1/10 ps^{-1} for the excited-state decay rate of the duplex dimer structure. The right panel of **Figure S3.3** shows that, as expected, SAS_3 derived from the global target analysis exhibits overall good agreement with the TA spectrum of the monomer measured from the monomer-only solution.

In conclusion, a three-component kinetics scheme, including two components to account for the sequential decay of duplex dimer structures and a third component to account for the parallel decay of a small subpopulation of monomers, is that which best describes the TA of the no-salt type 1 solution excited at 675 nm.

Section S4: Holliday junction Cy5 monomer excited-state lifetime

Time-resolved fluorescence measurements were performed to determine the excited-state lifetime of Cy5 monomer templated via a DNA Holliday junction. Specifically, time-correlated single photon counting (TCSPC) measurements were conducted on a solution of DNA Holliday junction structures where only one strand, in this case the D strand, is labeled with Cy5 (what we labeled as the Cy5 monomer). The solution was excited at 650 nm and fluorescence was detected at 680 nm, resulting in the data shown in **Figure S4.1**. A biexponential function was necessary to fit these data. The Cy5 monomer excited-state lifetime was determined to be ~1.5 ns by taking the amplitude-weighted average of the two decay constants from the biexponential fit. The excited-state lifetime measured here for the Holliday junction Cy5 monomer is similar to previously reported lifetimes of 1.3 and 1.5 ns for duplex DNA templated Cy5 monomer.[1]

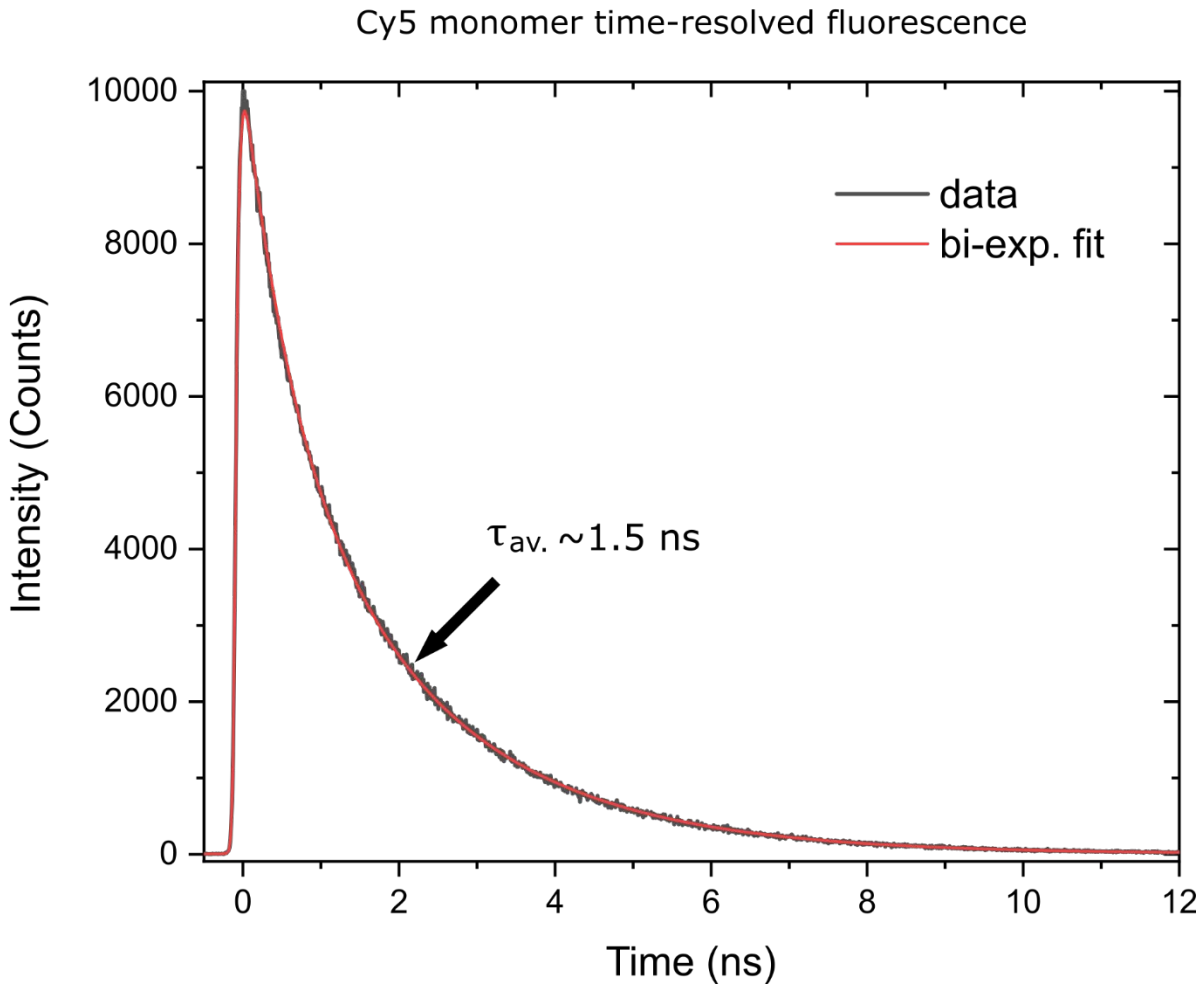

Figure S4.1. TCSPC results for Holliday junction Cy5 monomer. The data are shown in black and the fit is shown in red.

Section S5: Two-component global target analysis of transient absorption of high-salt type 1 solution excited at 555 nm

The transient absorption (TA) collected for the high-salt type 1 (largely Holliday junction tetramer) solution excited at 555 nm (and shown in **Figure 3** in the main text) was subject to global target analysis according to a two-component kinetic scheme shown in **Figure S5.1**. In this supporting section, we discuss the physical and mathematical basis for the two components used to model the TA dataset.

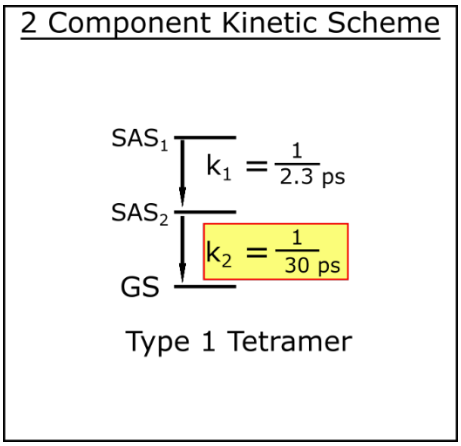

Figure S5.1. The two-component kinetic scheme used in the global target analysis of the transient absorption of the high-salt type 1 aggregate solution excited at 555 nm. Two components are included to account for sequential dynamics of the type 1 tetramer structures. Each species associated spectrum, SAS_n, is assigned a rate constant, k_n.

First, we provide mathematical justification for the two-component kinetic scheme. Global target analysis was first performed using a single component since previous TA measurements exciting and probing at 560 nm exhibited essentially single exponential relaxation kinetics.[1] The top row of **Figure S5.2** shows kinetics traces at probe wavelengths of 560 and 605 nm and associated fits and residuals when the data are modeled according to the one-component kinetic scheme.

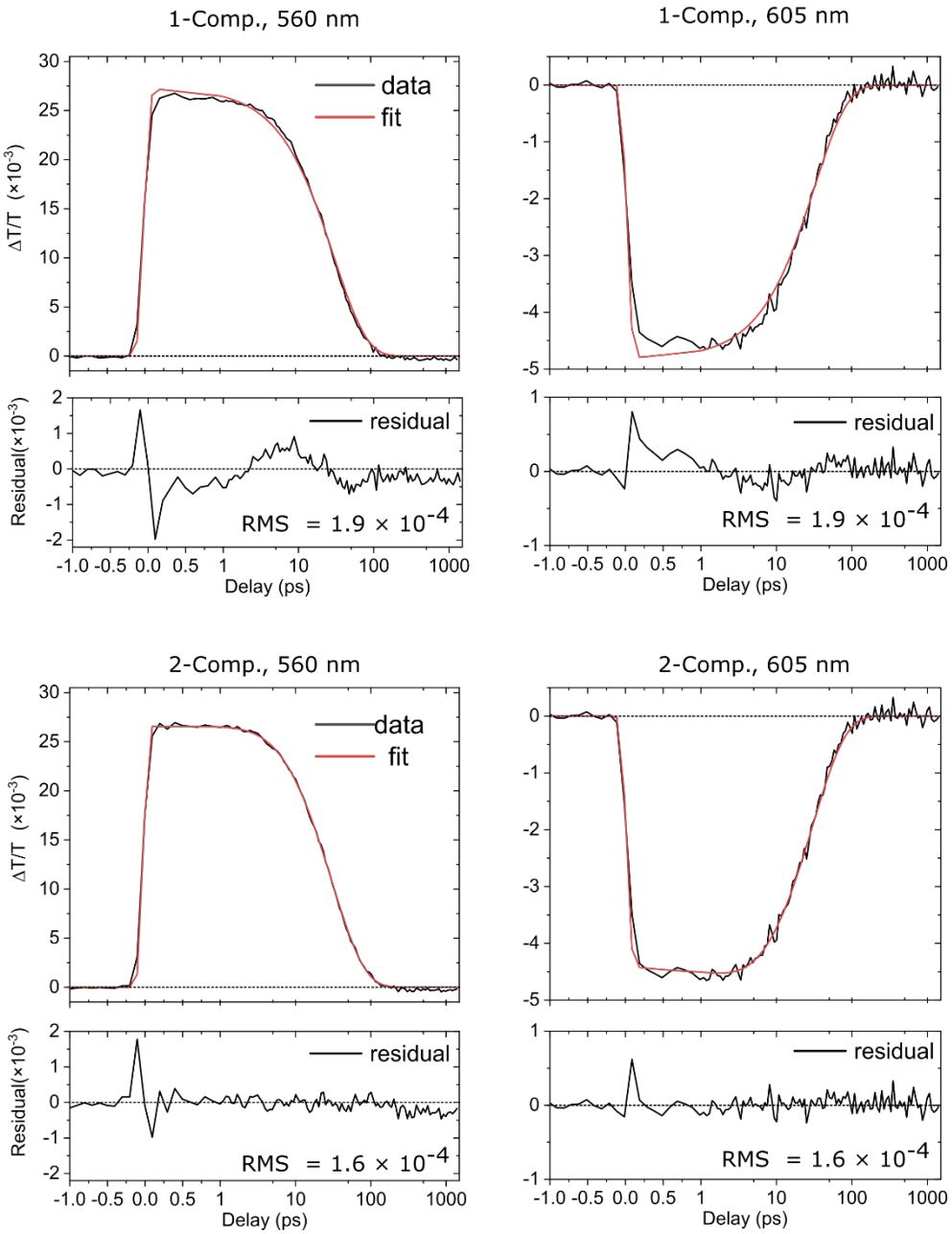

Figure S5.3. Selected kinetics traces (black) and fits (red) taken at 560 and 605 nm, which have been assigned to ground state bleach and the excited state absorption features, respectively, of the type 1 tetramer structure. (Top left) 560 nm kinetics trace and one component fit of the data with the fit residual plotted below. (Top right) 605 nm kinetics trace and one component fit of the data with the fit residual plotted below. (Bottom left) 560 nm kinetics trace and two component fit of the data with the fit residual plotted below. (Bottom right) 605 nm kinetics trace and two component fit of the data with the fit residual plotted below.

The probe wavelengths of 560 and 605 nm were chosen as they correspond to ground-state bleach (GSB) and excited-state absorption (ESA) features, respectively, of the Holliday junction H-tetramer structure (see **Figure 4B** of the main text). The single-component fit of the main GSB

kinetics trace at 560 nm exhibits overall good agreement, though there appear to be some deviations between the kinetics trace and the fit particularly on the sub-100-ps timescale. Deviations on the sub-100-ps timescale are also evident when comparing the fit to the kinetics trace corresponding to the ESA band at 605 nm. To account for these deviations, an additional component was added to the kinetics scheme used to model the data. The results of a global target analysis performed with a two-component kinetic scheme are shown in the bottom row of **Figure S5.2**. Clearly, the agreement between the kinetics traces and fits are considerably improved at both 560 and 605 nm. Consistent with this observation, the RMS value is smaller and the residuals show very little structure compared with those associated with the one-component kinetic scheme. We thus conclude that two components are mathematically justified to fit the transient absorption of the high-salt type 1 solution excited at 555 nm.

Having justified the two-component kinetic scheme mathematically, we next discuss the physical origin of the two components. As discussed above in **Section S.3**, a two-component kinetic scheme could be due to two components decaying either in sequence or in parallel. **Figure S5.3** displays species associated spectra (SAS) returned from the global target analysis using sequential and parallel two-component kinetics schemes.

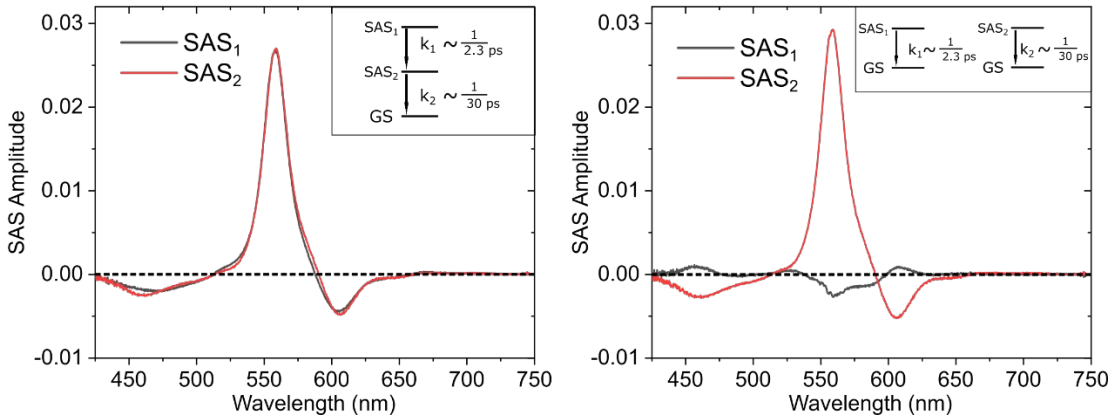

Figure S5.3. Species-associated spectra (SAS) resulting from a global target analysis of the TA of the high-salt type 1 solution excited at 555 nm, with the global target analysis assuming either a sequential (Left) or parallel (Right) two-component kinetic scheme. The kinetics schemes are shown in the insets.

In the case of the sequential two-component kinetics scheme, the two SAS—SAS_1 and SAS_2—are overall very similar. Slight differences in the spectra are observed, mostly in the vicinity of the ESA bands at wavelengths lower and higher than the main GSB feature at 560 nm. In the case of the parallel two-component kinetics scheme, in contrast, SAS_1 and SAS_2 are drastically different. SAS_2 clearly resembles what we expect for the TA signal of the type 1 H-tetramer structure, while SAS_1 appears to resemble a much smaller amplitude mirror image of SAS_2. Given that it is unlikely that an additional aggregate structure is present in the high-salt type 2 solution that exhibits a TA signal largely reminiscent of a mirror image of the TA signal of the Holliday junction H-tetramer

structure, we conclude the result is not physical and therefore rule out the parallel two-component kinetics scheme.

Having determined that the sequential two-component kinetics scheme is that which best describes the TA of the high-salt type 2 solution excited at 555 nm, we conclude this section with a brief discussion of the physical nature of the two components in the sequential two-component kinetics scheme. As for the duplex dimer (**Section S3**), we assign SAS_1 to the vertically excited state, and SAS_2 to the excited state following some form of relaxation. As shown in **Figure S5.1**, values of 1/2.3 and 1/30 ps^{-1} are derived for the rate constants k_1 and k_2 associated with SAS_1 and SAS_2, respectively. Critical for this work is k_2, which is the excited-state decay rate, i.e., direct relaxation to the ground state, and has a value of 1/30 ps^{-1}.

Section S6: Five-component global target analysis of transient absorption of high-salt type 1 solution excited at 660 nm

The transient absorption (TA) data collected for the high-salt type 1 solution excited at 660 nm (and shown in main text **Figure 3E-H**) was subject to global target analysis according to the five-component kinetic scheme shown in **Figure S6.1**. In this supporting section, we first describe why a four-component kinetics scheme represents an appropriate initial basis for modeling the TA data and then proceed to provide mathematical justification for the five-component kinetic scheme needed to fully model the TA data.

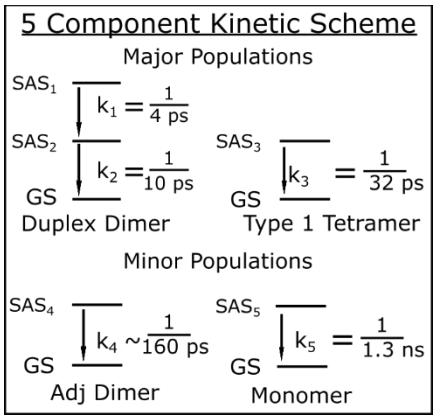

Figure S6.1. The five-component kinetic scheme used in the global target analysis of the transient absorption of the high-salt type 1 aggregate solution excited at 660 nm. The first three components (associated with k_1 – k_3) account for the two main subpopulations of duplex dimer structures, which exhibit biexponential sequential kinetics in the model, and type 1 tetramer structures, which exhibit monoexponential kinetics in the model. The last two components, associated with k_4 and k_5, account for small subpopulations of adjacent dimers and Cy5 monomers, respectively. The rate constants for all components except the adjacent dimer (k_4) were fixed to the values measured previously as indicated by an equals sign. The rate constant associated with the fourth kinetic component, k_4, was not fixed. Each species associated spectrum, SAS_n, is assigned a rate constant, k_n.

We began by fitting the TA data globally according to a four-component kinetic scheme. The use of a four-component kinetic scheme is physically justified based on previous characterizations of type 1 solutions.[1,2] Specifically, Cannon *et al.* showed that the high-salt type 1 solution contains primarily type 1 tetramers as well as subpopulations of duplex dimers; Huff *et al.* showed that the high-salt type 1 solution also contains a small subpopulation of monomers. All three populations absorb at the 660 nm excitation wavelength used to perform the measurements and so will contribute to the TA signal. A four-component kinetic scheme is therefore justified physically because each component can be assigned to one of these physical populations. We assign two components to a subpopulation of duplex dimer structures. These two components were assigned in accordance with the two-component kinetics scheme determined for the 'pure' duplex

dimer in **Section S3**. The first two rate constants, i.e., k_1 and k_2, were thus fixed to 1/4 and 1/10 ps^{-1}, respectively. A third component was assigned to a subpopulation of type 1 tetramer structures. Here, only one component was assigned because the difference in amplitude between the two components in the two-component kinetics scheme associated with 'pure' type 1 tetramer structures was very small (**Section S5**). The rate constant associated with this component was fixed to 1/32 ps^{-1} since this value was returned by a single component fit to the 'pure' TA of the Holliday junction H-tetramer (see one-component fits to kinetics traces in **Figure S5.2**). Lastly, a fourth component was included to account for monomer contribution to the TA data. The rate constant associated with this component was fixed to 1/1.3 ns^{-1} (**Section S4**).

Having justified the four-component kinetic scheme, we next provide mathematical justification for a fifth component. **Figure S6.2** plots kinetics traces compared along with fits from a global target analysis of the TA data according to four- and five-component kinetics schemes.

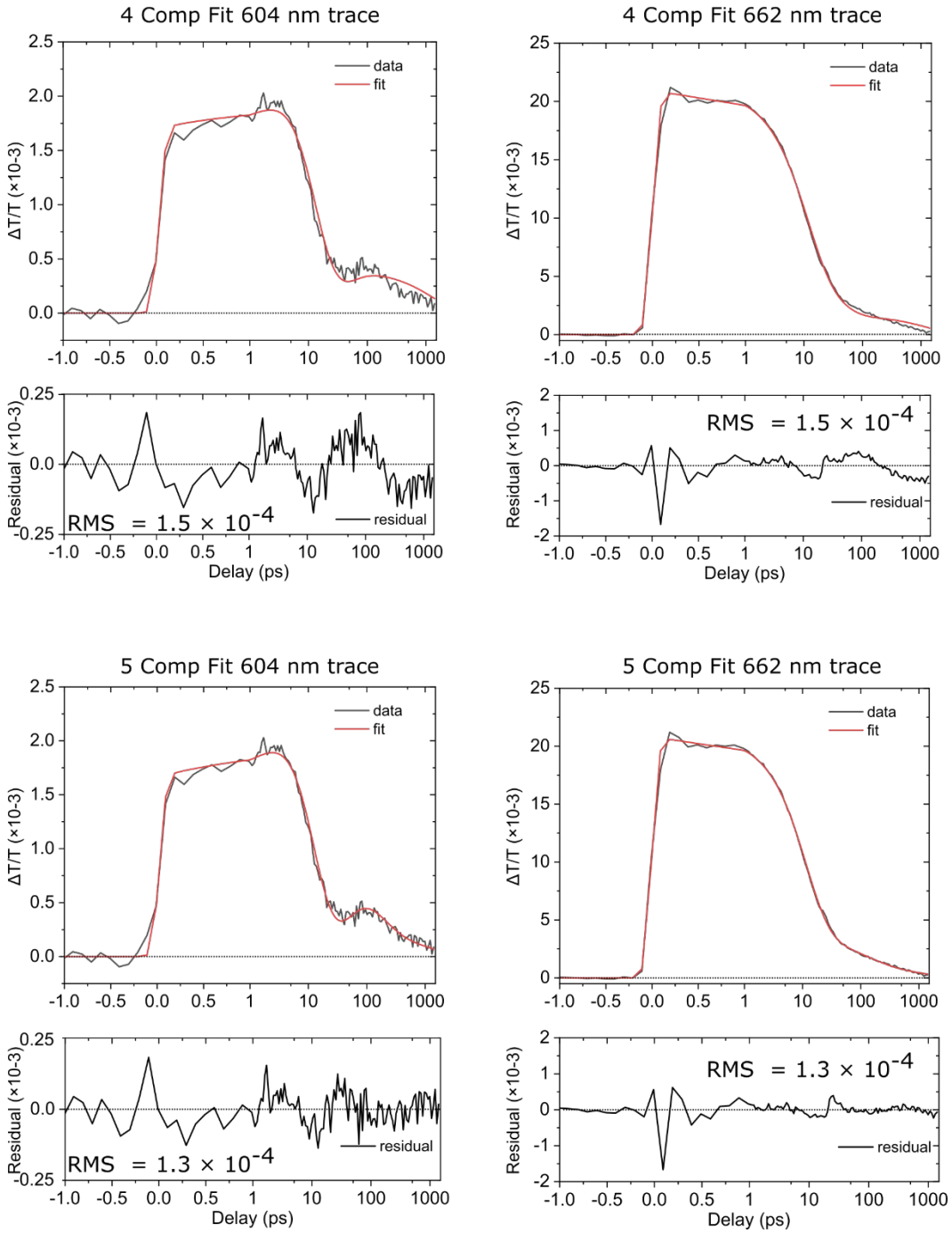

Figure S6.2. Selected kinetics traces (black) and fits (red) taken at 604 and 662 nm. The 604 nm trace overlaps with the ESA band of the type 1 tetramer and a secondary ground state bleach band of the duplex dimer and the trace at 662 nm overlaps primarily with the primary ground state bleach of the duplex dimer. (Top left) 604 nm kinetics trace and four-component fit of the data with the fit residual plotted below. (Top right) 662 nm kinetics trace and four-component fit of the data with the fit residual plotted below. (Bottom left) 604 nm kinetics trace and five-component fit of the data with the fit residual plotted below. (Bottom right) 662 nm kinetics trace and five-component fit of the data with the fit residual plotted below.

We first focus on the four-component fits displayed in the top row of **Figure S6.2**, specifically the fit to the 662 nm kinetics trace. We see reasonably good agreement between the data and the fit at early times, but the fit begins to deviate beyond ca. 1 ps as can be seen from the structure that appears in the residual plot. The disagreement between data and fit is even more apparent in the four-component fit of the 604 nm kinetics trace where again we see appreciable deviation past 1 ps. With clear deviations between the data and the fit evident, particularly in the additional structure in the residual, we performed global target analysis with an additional fifth component. The results of the five-component global target analysis are plotted at the bottom half of **Figure S6.2**. With the other four components fixed to their respective values listed above, the rate constant of the added component was derived to be 1/160 ps^{-1}. Clearly, including an additional component improves the overall agreement between the data and the fit. This is evident by visual inspection of the data and the fit, the reduced RMS of the data with the fit (decreasing from 1.5×10^{-4} to 1.3×10^{-4}), along with the reduction of structure in the residual plots. Thus, we conclude that five components are mathematically justified.

Having shown that a five-component kinetic scheme best describes the TA of the high-salt type 1 solution excited at 660 nm, we conclude this supporting section with some discussion of the identity of the additional component. First, we must consider whether this component decays in parallel to the other components, or in sequence. The sequential decay scenario can be dismissed immediately on the basis that the 1/160 ps^{-1} rate constant derived above for the additional component does not match with any of the rate constants associated with the populations known to be present in solution (e.g., duplex dimer structures, Holliday junction H-tetramer structures, and monomer). We therefore conclude that the additional component must decay in parallel with the other components, which implies an additional, previously unidentified aggregate subpopulation in the high-salt type 1 solution.

In order to aid in identifying this aggregate subpopulation, we next consider the species associated spectrum (SAS) of the additional component. **Figure S6.3** shows the SAS derived from the five-component kinetic scheme.

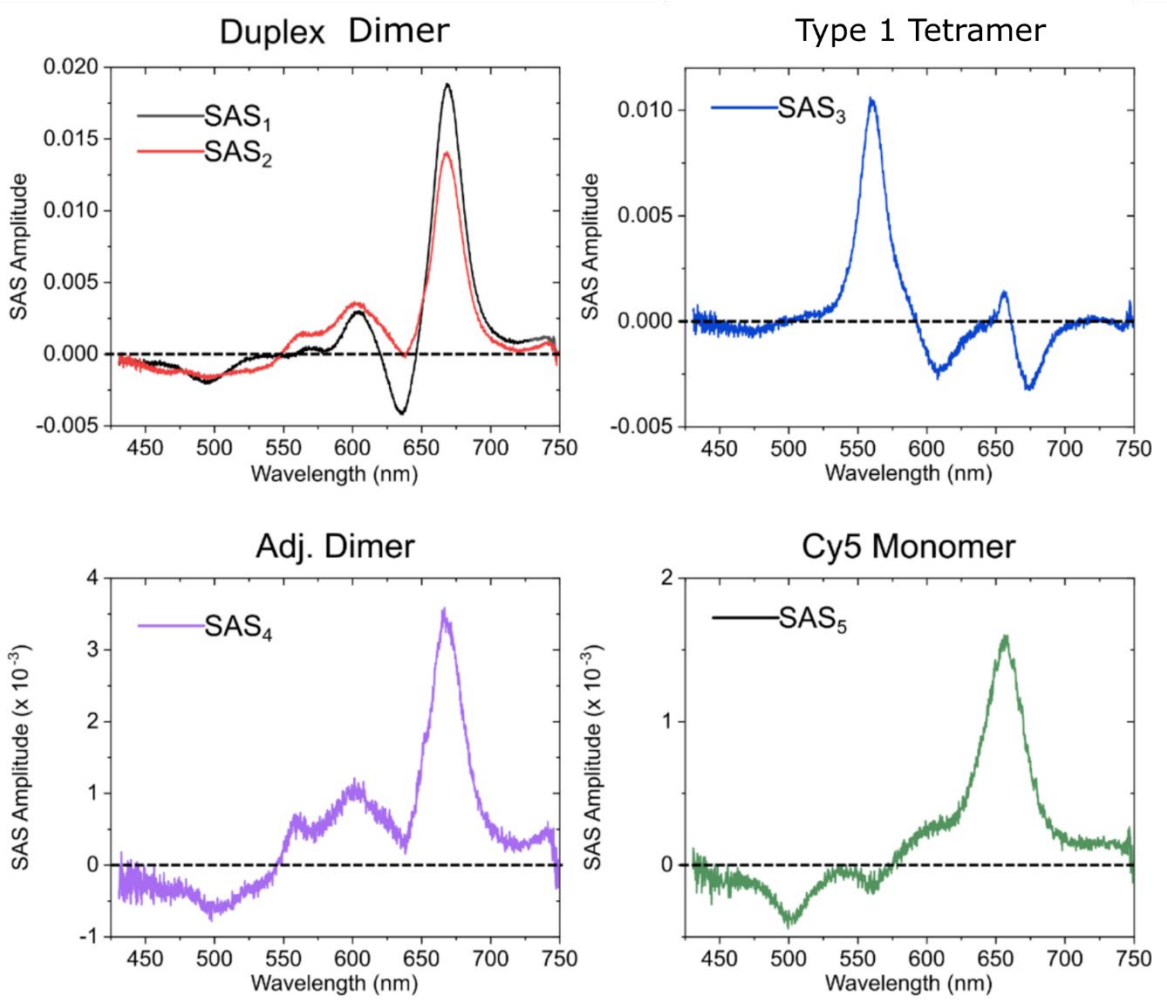

Figure S6.3. Species associated spectra (SAS) returned from the five-component global target analysis of the high-salt type 1 solution excited at 660 nm. (Top left) SAS_1 and SAS_2 account for the duplex dimer and correspond to the rate constants of 1/4 and 1/10 ps^{-1}, respectively. (Top right) SAS_3 which accounts for the Holliday junction H-tetramer and corresponds to the 1/32 ps^{-1} rate constant. (Bottom left) SAS_4 which accounts for the additional subpopulation of adjacent dimer structures with a rate constant of 1/160 ps^{-1}. See the last paragraph of this supporting section for more about the assignment of SAS_4. (Bottom right) SAS_5 which accounts for the Cy5 monomer subpopulation and corresponds to the 1/1.3 ns^{-1} rate constant.

Upon initial inspection, SAS_4, which is associated with the 1/160 ps^{-1} rate constant, appears to resemble SAS_2 associated with duplex dimer structure. Even though the spectra look similar, however, the components exhibit large differences in their relaxation rate constants. Specifically, k_2 associated with SAS_2 has a value of 1/10 ps^{-1}, which is nearly an order of magnitude faster than the k_4 associated with the additional component. If we also compare the rate constant and SAS of the additional component to those derived for type 2 aggregates, specifically the adjacent dimer structure, even better agreement is observed. **Figure S6.4** plots together the normalized SAS

assigned to the long-lived adjacent dimer subpopulation and the normalized SAS of the additional component.

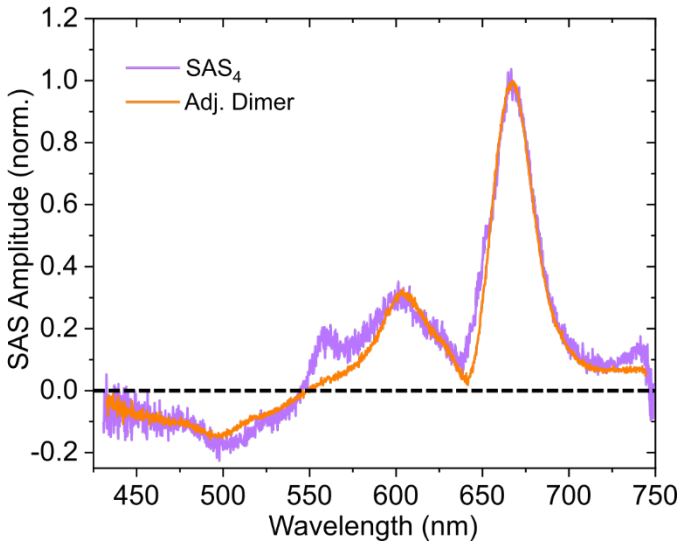

Figure S6.4. Normalized plots of the fourth species-associated spectrum (SAS), i.e., SAS_4, returned from the five-component global target analysis of the high-salt type 1 solution excited at 660 nm (purple), and the SAS assigned to adjacent dimer structures (orange). SAS_4 is associated with a 1/160 ps^{-1} rate constant, and the adjacent dimer structures are associated with a 1/240 ps^{-1} rate constant.

The two spectra show very close agreement. The positive- and negative-going signals, i.e., ground-state bleach and excited-state absorption features, respectively, show excellent agreement in position and relative amplitudes. Additionally, the rate constants of 1/160 ps^{-1} and 1/240 ps^{-1} associated with the additional component and the adjacent dimer structure, respectively, are very similar. Given the similarity of the SAS and rate constants, we therefore assign the additional component to a previously unidentified subpopulation of adjacent dimer structures present in the high-salt type 1 solution.

Section S7: Four-component global target analysis of transient absorption of transverse dimer solution excited at 600 nm

The spectrotemporal transient absorption (TA) dataset collected for the type 2 transverse dimer solution excited at 600 nm was subject to global target analysis according to a four-component kinetic scheme shown in **Figure S7.1**. In this supporting section, we discuss the physical and mathematical basis for the four components used to model the TA dataset.

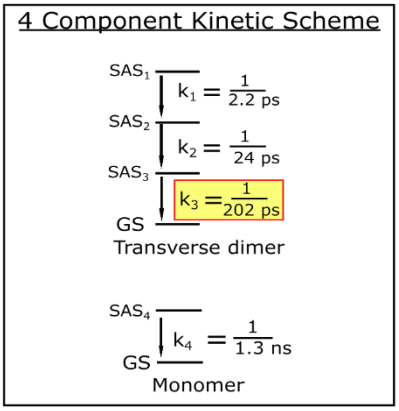

Figure S7.1 The four-component kinetic scheme used in the global target analysis of the transient absorption of the transverse dimer solution excited at 600 nm. Two of the three components associated with aggregates account for two subpopulations present in the solution, a large sub-population of transverse dimer structures and a small subpopulation of monomers. The other two components, k_1 and k_2, account for sequential dynamics of the transverse dimer subpopulation. A fourth component associated with a small subpopulation of monomers had its excited-state decay rate (k_4) fixed to a value of 1/1.3 ns^{-1}.

We initially attempted to model the data with a single component, then proceeded to incorporate additional components until a sufficient fit was achieved. The kinetics trace of the main ground state bleach feature at 600.5 nm (see **Figure 5** in the main text) along with a single component fit is shown in **Figure S7.2** (see left panel). The fit residual exhibits considerable structure which prompted the addition of a second component. The right panel of **Figure S7.2** shows the same kinetics trace taken at 600.5 nm with a two component fit superimposed. Clearly, the residual of the two component fit is reduced considerably at all timescales except at the time origin.

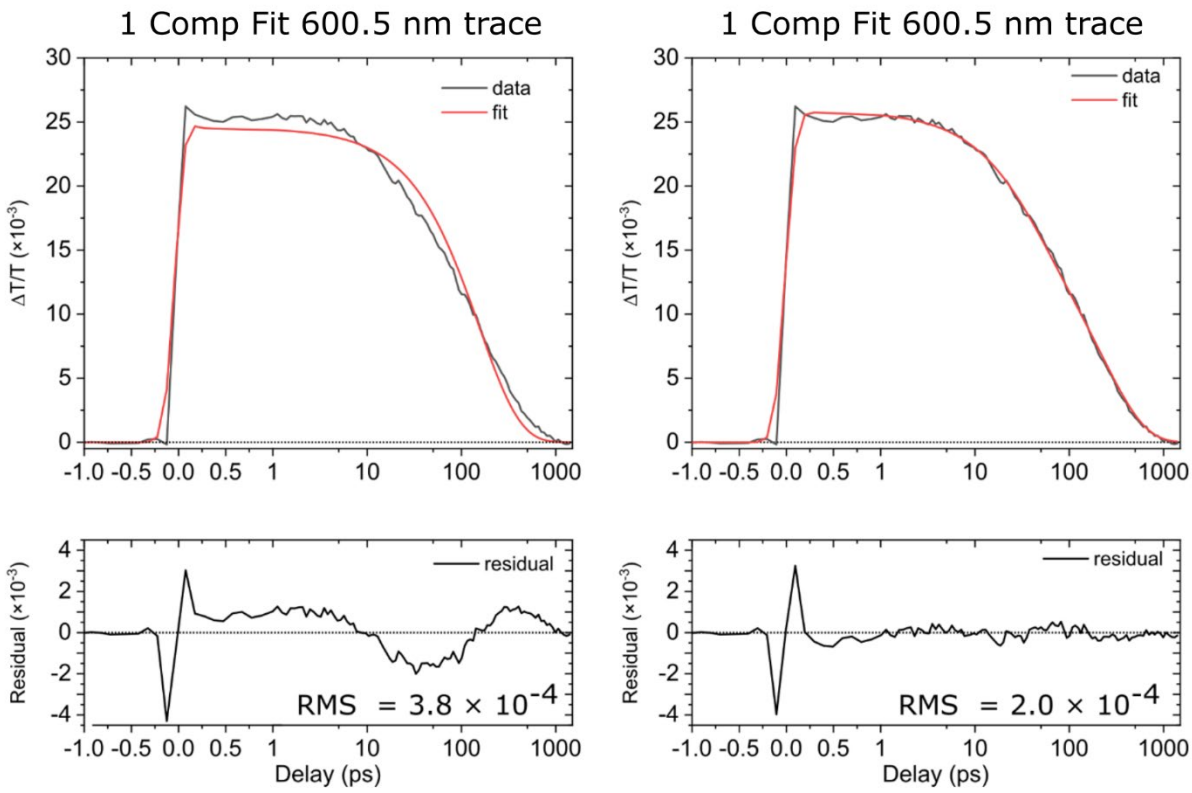

Figure S7.2 Selected kinetics traces (black) and fits (red) taken at 600.5 nm, which is in the vicinity of the strongest ground-state bleach feature of the transverse dimer solution. (Left) 600.5 nm kinetics trace and one-component fit of the data with the fit residual plotted below. (Right) 600.5 nm kinetics trace and two-component fit of the data with the residual plotted below.

While the two-component model fit the data well at 600.5 nm, i.e., a single kinetics trace, the fit to the data was not as good at other wavelengths modeled in the global analysis. For example, the residual of the kinetics trace and two-component fit at 667 nm (**Figure S7.3**, left panel) exhibits considerable structure at long time delays, i.e., beyond ~10 ps. This prompted the addition of a third component to the global target analysis. To better model the data, we included a third component whose rate constant (k_3) was fixed to that of the monomer (i.e., k3 ~ 1/1.3 ns^{-1}; see e.g. **Section S4**). This was justified for the following reasons: (i) the long-time TA spectrum from the raw data well matches that of the monomer, (ii) at 600 nm excitation, the monomer is expected to absorb appreciably, and (iii) the strongest ground-state bleach feature of the monomer appears at 667 nm (i.e., the wavelength at the focus of the present analysis). The right panel of **Figure S7.3** shows the kinetics trace at 667 nm plotted with the three-component fit. The fit at 667 nm is considerably improved by adding an additional monomer component as can be seen by comparing the residuals at long times in **Figure S7.3**.

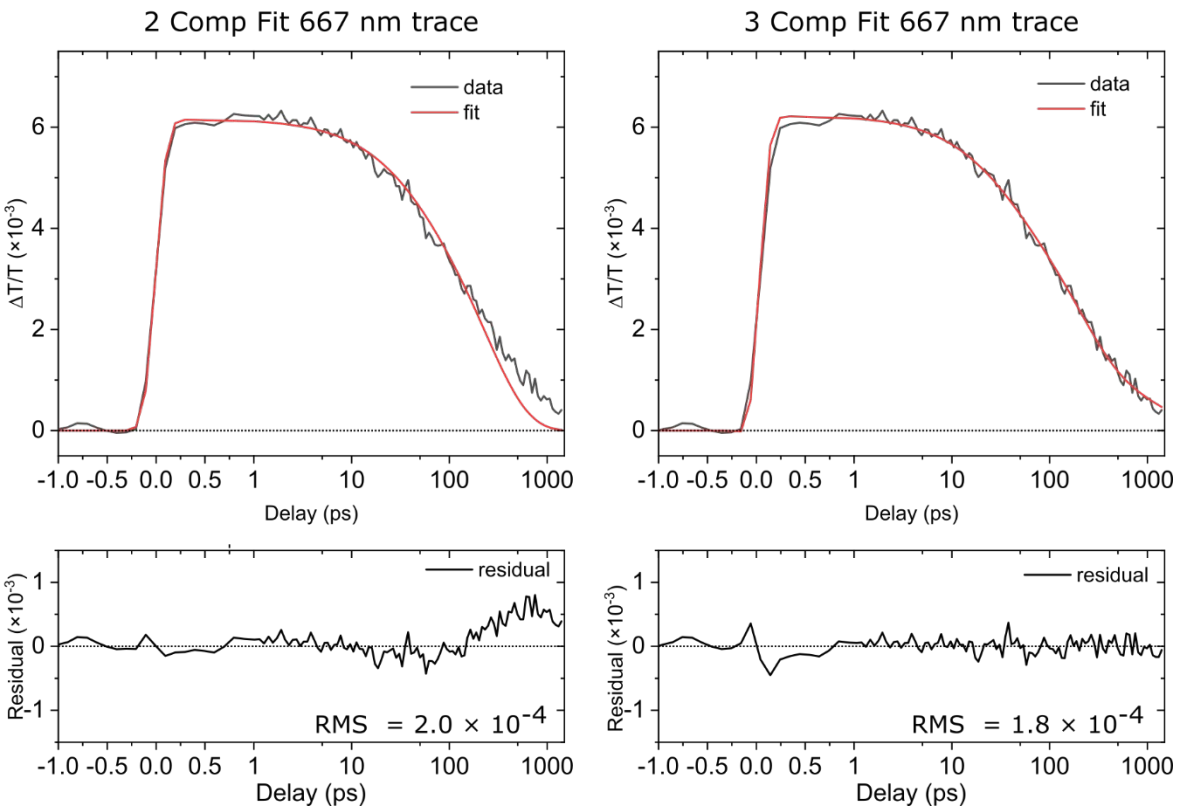

Fig S7.3 Selected kinetics traces (black) and fits (red) taken at 667 nm, which is in the vicinity of the strongest ground-state bleach of the Cy5 monomer. (Left) 667 nm kinetics trace and two-component fit of the data with the fit residual plotted below. (Right) 667 nm kinetics trace and three-component fit of the data with the residual plotted below.

Finally, a fourth component was incorporated into the model to improve the fit at delay times shorter than 100 ps. **Figure S7.4** shows the kinetics trace at 500 nm and the three-component fit superimposed. The residual of the fit, shown below the kinetics trace plot, exhibits structure, especially for delays shorter than ~ 100 ps. A fourth component was included in the kinetic scheme to account for these rapid dynamics. The fit is significantly improved as can be seen in the right panel of **Figure S7.4** which shows the 500 nm kinetics trace and four-component fit. The residual, shown in the bottom right panel of **Figure S7.4**, exhibits no structure. We therefore conclude based on the good global fit and resulting improved RMS that kinetic components are the minimum required to adequately fit this spectrotemporal dataset.

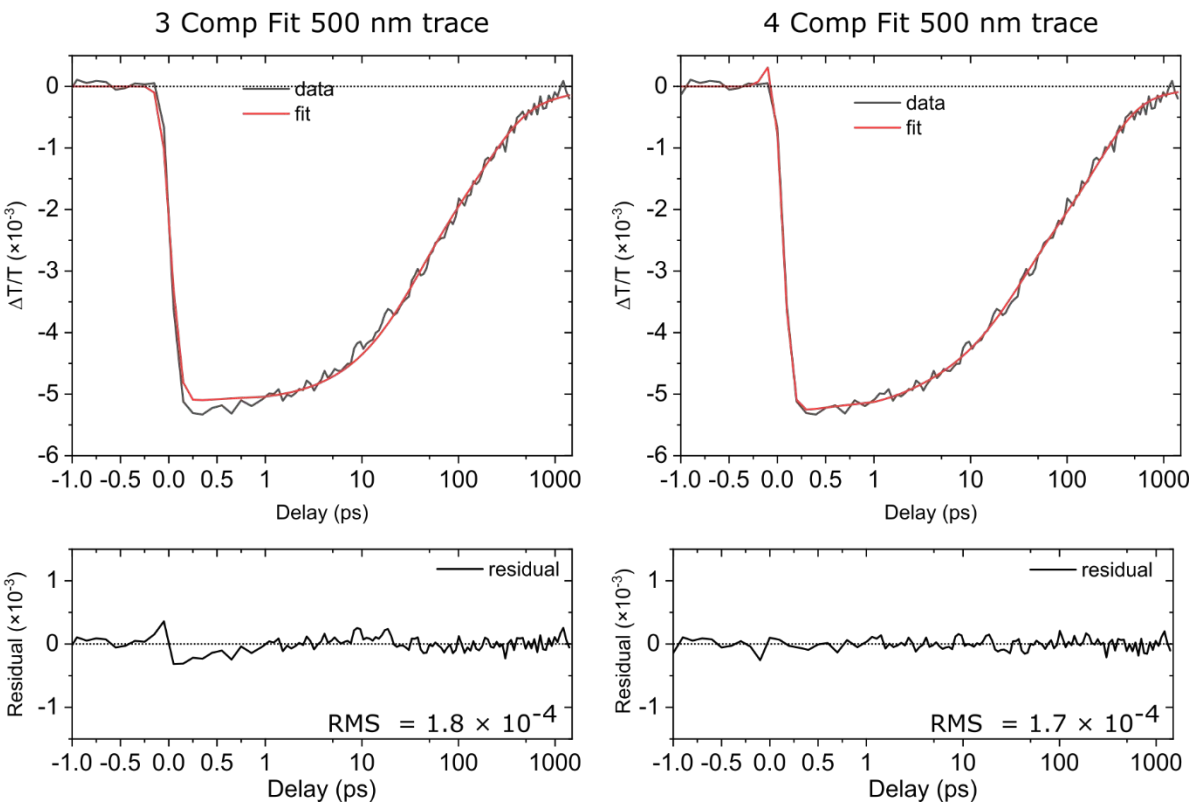

Figure S7.4 Selected kinetics traces (black) and fits (red) taken at 500 nm, which is in the vicinity of a strong excited-state absorption band resulting from the aggregates. (Left) 500 nm kinetics trace and three-component fit of the data with the fit residual plotted below. (Right) 500 nm kinetics trace and four-component fit of the data with the residual plotted below.

Having justified the presence of four components, we next discuss the physical assignment of the different components and their decay pathways (**Figure S7.1**). We begin the discussion with the fourth component, which we assigned to a small subpopulation of monomers and whose decay rate we fixed to $k_4 \sim 1/1.3$ ns^{-1}. As noted already in a preceding paragraph, the small subpopulation of monomers was selected to decay in parallel with the other three components because the 600 nm excitation condition for the experiment can simultaneously excite both the primary aggregate population (see e.g. the steady-state absorption spectrum) along with a small subpopulation of monomers, which also absorb in the vicinity of 600 nm. In support of this model, the fourth species-associated spectrum (SAS) or SAS_4, which corresponds to the component associated with k_4, largely resembles the TA spectrum of the monomer (**Figure S7.5**).

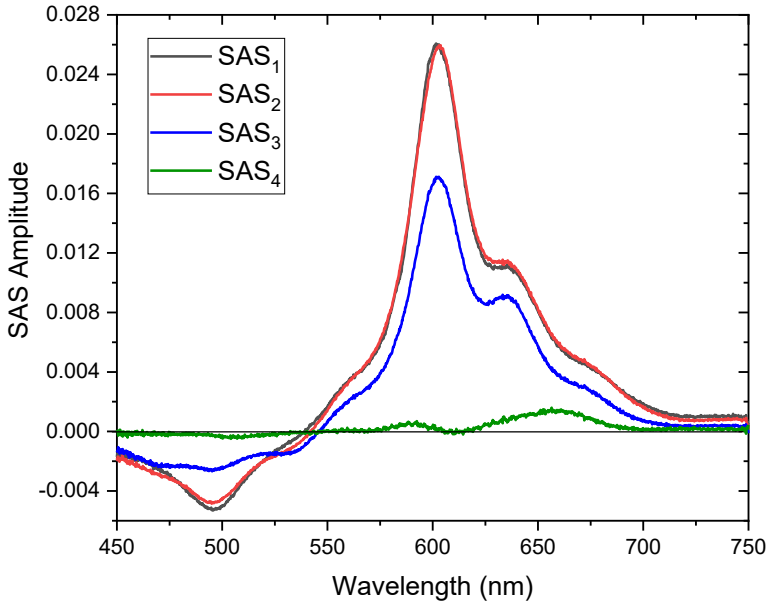

Figure S7.5 Species-associated spectra resulting from a global target analysis of the TA of the type 2 transverse dimer with the global target analysis assuming a four-component kinetic scheme. SAS_1, SAS_2, and SAS_3 are assigned to the sequential decay of the transverse dimer. SAS_4 is assigned to the monomer subpopulation.

With respect to the remaining three components, since we found the transverse dimer solution to be largely homogeneous with respect to aggregates (see e.g. **Figure 6** in the main text), we used a model where the remaining three components decay in sequence (see e.g. **Figure S7.1**). SAS_1, SAS_2, and SAS_3 derived from the model, with decay rate constants (k_1, k_2, and k_3) of ~1/2, 1/20, and 1/202 ps^{-1}, are shown in **Figure S7.5**. The primary focus of this work is the excited-state decay rate of the transverse dimer, which we assign to k_3 and which has a value of ~1/202 ps^{-1}.

Section S8: Four-component global target analysis of transient absorption of adjacent dimer solution excited at 675 nm

The spectrotemporal transient absorption (TA) dataset collected for the adjacent dimer solution excited at 675 nm was subject to global target analysis according to a four-component kinetic scheme shown in **Figure S8.1**. In this supporting section, we discuss the physical and mathematical basis for the four components used to model the TA dataset.

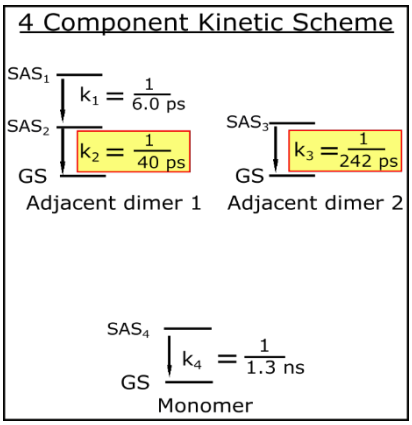

Figure S8.1 The four-component kinetic scheme used in the global target analysis of the transient absorption of the adjacent dimer solution excited at 675 nm. Three of the four components correspond to subpopulations in the solution, namely, a short-lived adjacent dimer, a long-lived adjacent dimer, and a small subpopulation of monomers. Two of the three aggregate components included in the kinetic scheme account for sequential dynamics in the short-lived adjacent dimer subpopulation. A fourth component associated with a small subpopulation of monomers had its excited-state decay rate (k_4) fixed to a value of 1/1.3 ns^{-1}. Each species associated spectrum, SAS_n, is assigned a rate constant, k_n.

The data were first analyzed globally using the simplest model including a single component. The resulting fit and residual taken from the main ground-state bleach feature at 671 nm (see **Figure 5** in the main text) is shown in the left column of **Figure S8.2**. It is clear from the poor fit and structure in the residual that the single-component kinetic scheme does not model the data well. Accordingly, a second component was added to the model. The fit at 671 nm was substantially improved as can be seen in the right column of **Figure S8.2**, although residual structure is still evident on the >10 ps timescale.

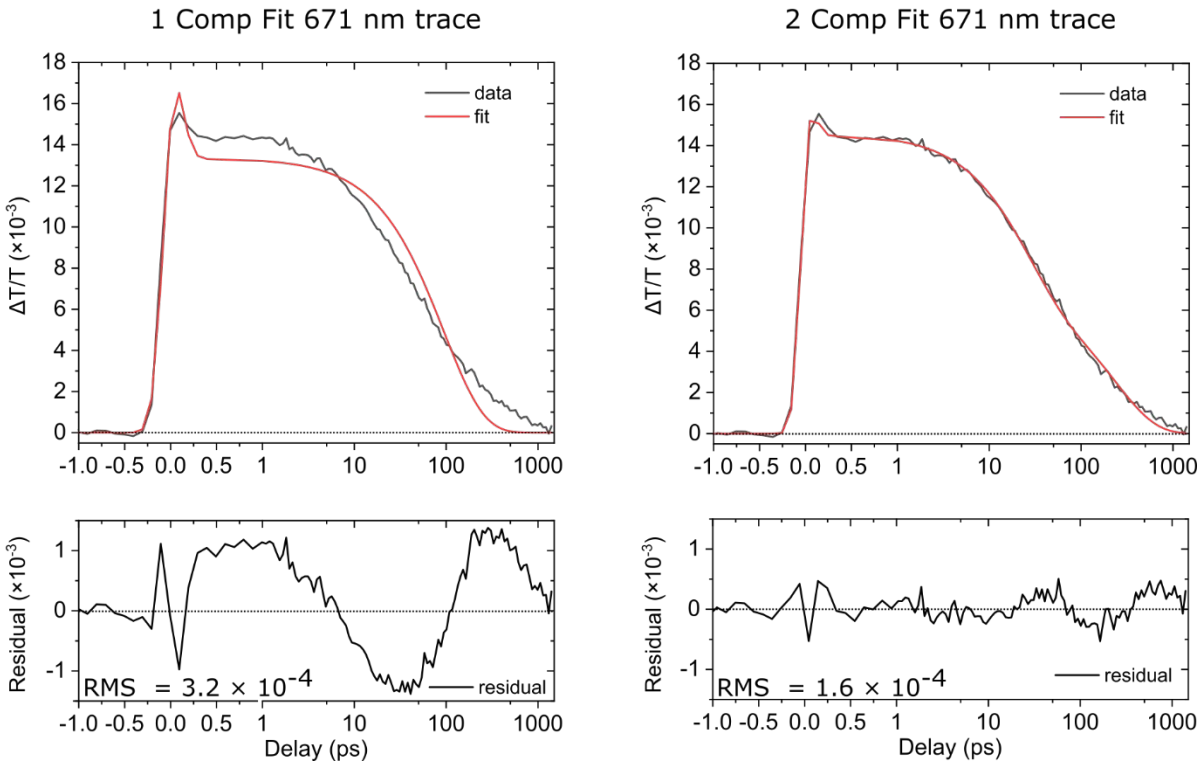

Figure S8.2 Selected kinetics traces (black) and fits (red) taken at 671 nm, which corresponds to the primary ground-state bleach feature of the adjacent dimer solution. (Left) 671 nm kinetics trace and one-component fit of the data with the fit residual plotted below. (Right) 671 nm kinetics trace and two-component fit of the data with the residual plotted below.

While two exponentials fit the main bleach trace at 671 nm reasonably well, there are other wavelengths where the global fit does not model the data well. Specifically, the fit to the data at the second-most intense ground-state bleach feature at ca. 608 nm (see **Figure S8.3,** left) is noticeably poor. This suggests that an additional component is necessary to accurately model the data. Performing the analysis with an additional, third component resulted in an improved fit (**Figure S8.3**, right). Remaining structure in the residual, however, especially noticeable at delays shorter than 1 ps, suggests a fourth component is warranted. By including a fourth component, the fit at 608 nm is substantially improved such that there is no longer any obvious structure evident in the residual (**Figure S8.4**, right). We therefore conclude that four components are sufficient to model these data.

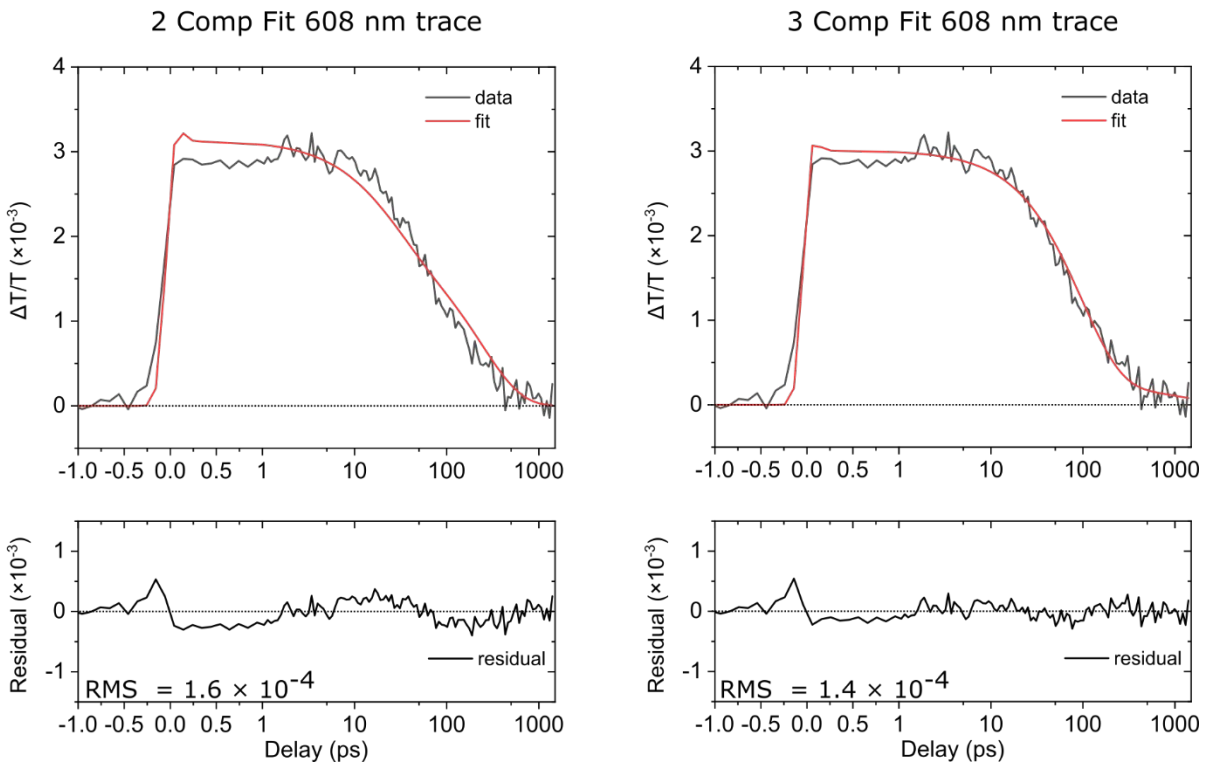

Figure S8.3 Selected kinetics traces (black) and fits (red) taken at 608 nm, which corresponds to the second-most intense ground-state bleach feature of the adjacent dimer solution. (Left) 608 nm kinetics trace and two-component fit of the data with the fit residual plotted below. (Right) 608 nm kinetics trace and three-component fit of the data with the residual plotted below.

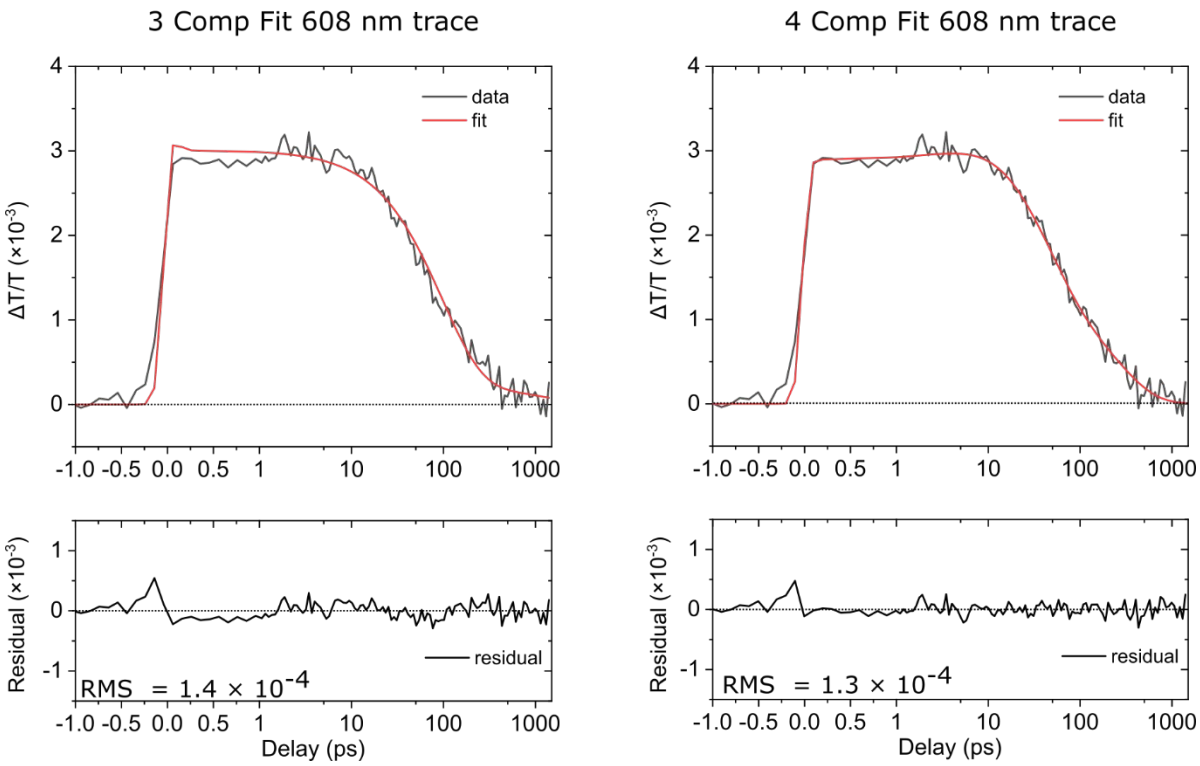

Figure S8.4 Selected kinetics traces (black) and fits (red) taken at 608 nm, which corresponds to the second-most intense ground-state bleach feature of the adjacent dimer solution. (Left) 608 nm kinetics trace and three-component fit of the data with the fit residual plotted below. (Right) 608 nm kinetics trace and four-component fit of the data with the residual plotted below.

Having demonstrated that four components are needed to fit the TA of the adjacent dimer solution, we now discuss and assign the different components and decay pathways shown in the kinetic scheme in **Figure S8.1**. First, as we argued in **Section S7**, we assign the fourth component to a subpopulation of monomers, and fix its decay rate $k_4 \sim 1/1.3$ ns^{-1}. Further justifying the assignment, SAS_4 derived from the model strongly resembles the monomer TA spectrum (**Figure S8.5**).

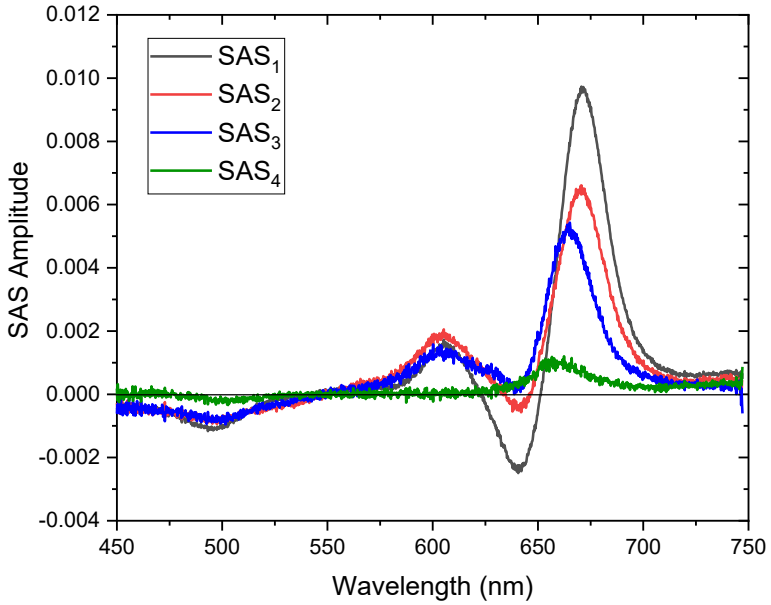

Figure S8.5 Species-associated spectra resulting from a global target analysis of the TA of the type 2 adjacent dimer solution according to the four-component kinetic scheme shown in **Figure S8.1**. SAS_1 and SAS_2, are assigned to two components associated with a short-lived adjacent dimer subpopulation, with the two components decaying in sequence. SAS_3 is assigned to a long-lived adjacent dimer subpopulation decaying in parallel. SAS_4 is assigned to a small subpopulation of monomers also decaying in parallel.

Next, we discuss the first three components, i.e., SAS_1, SAS_2, and SAS_3, and their associated decay rate constants, i.e., k_1, k_2, and k_3. First, we argue based on the observation of considerable heterogeneity in this solution (see **Figure 6** in the main text) that a parallel kinetic scheme is necessary to model these data. Thus, we can rule out a fully sequential kinetic scheme. Furthermore, we rule out the possibility that all components decay in parallel (which would indicate four subpopulations in the solution) because the decay associated spectrum related to SAS_1 is not physical for that case (see e.g. **Section S5** and ref. [3]). Thereafter, we must consider two remaining kinetic schemes where SAS_1 decays into SAS_2 (and SAS_3 decays in parallel) or, alternatively, where SAS_1 decays into SAS_3 (and SAS_2 decays in parallel). For the sake of simplicity, here and in subsequent sections, we consider only the former kinetic scheme where SAS_1 decays into SAS_2 (and SAS_3 decays in parallel). This is justified, as we have found SAS_1 and SAS_2 to generally exhibit the largest amplitude (**Figure S8.5**), and so, represent the primary aggregate sub-population in the solution.

According to these assignments, the four-component kinetic scheme shown in **Figure S8.1** was determined to be the most appropriate model. The corresponding SAS, shown in **Figure S8.5**, are assigned as a subpopulation of short-lived adjacent dimers that undergo sequential kinetics (i.e., SAS_1 and SAS_2), a subpopulation of long-lived dimer (i.e., SAS_3) that decays in parallel, and a small subpopulation of monomers (i.e., SAS_4) that also decay in parallel. Critically, we are able

to derive the excited-state decay kinetics of the short-lived and long-lived adjacent dimer subpopulations (i.e., k_2 and k_3), which we determine to be ~ 1/40 and 1/240 ps^{-1}, respectively.

Section S9: Four-component global target analysis of transient absorption of trimer solution excited at 560 nm

The spectrotemporal transient absorption (TA) dataset collected for the trimer solution excited at 560 nm was subject to global target analysis according to a four-component kinetic scheme shown in **Figure S9.1**. In this supporting section, we discuss the physical and mathematical basis for the four components used to model the TA dataset.

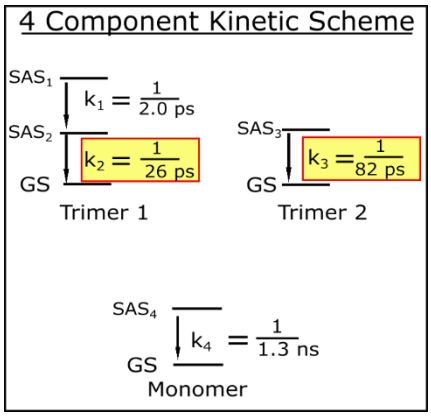

Figure S9.1 The 4 component kinetic scheme used for the trimer solution excited at 560 nm. Three of the four components correspond to subpopulations in the solution, namely a short-lived trimer, a longer-lived trimer, and a subpopulation of monomers. Two of the three aggregate components account for sequential dynamics in the short-lived adjacent dimer subpopulation. A fourth component associated with a small subpopulation of monomers had its excited-state decay rate (k_4) fixed to a value of 1/1.3 ns^{-1}. Each species associated spectrum, SAS_n, is assigned a rate constant k_n.

The data were first analyzed globally using the simplest model including a single component. The resulting fit and residual taken at 591 nm is shown in the left column of **Figure S.9.2.** It is clear from the poor fit and the presence of structure in the residual that the relaxation kinetics of the bleach are not monoexponential. Accordingly, a second component was included in the model. The two component fit at 591 nm was substantially improved as can be seen in the right panel of **Figure S9.2**, although residual structure can still be observed at delays > 10 ps.

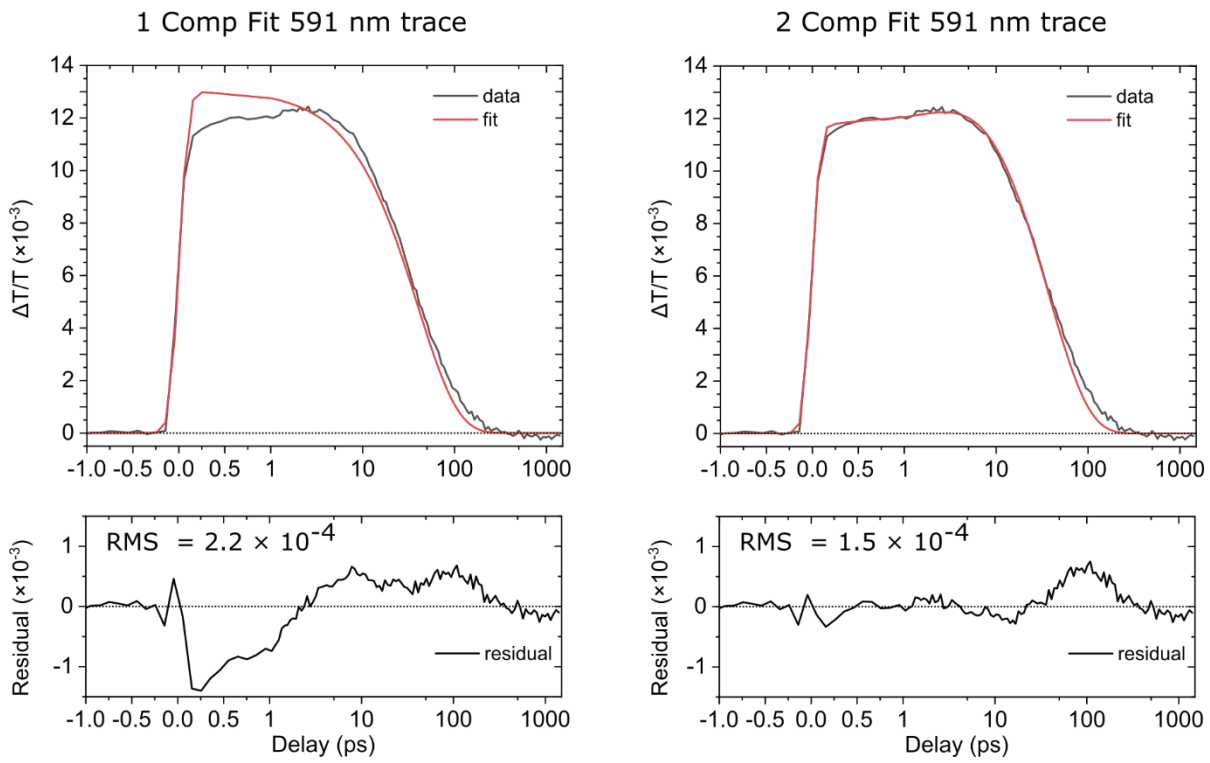

Figure S9.2 Selected kinetics traces (black) and fits (red) taken at 591 nm, which corresponds to a red-shifted shoulder of the most intense ground-state bleach feature of the trimer solution. (Left) 591 nm kinetics trace and one-component fit of the data with the fit residual plotted below. (Right) 591 nm kinetics trace and two-component fit of the data with the residual plotted below.

Since a two-component fit did not model the 591 nm decay satisfactorily at longer delays, the analysis was performed again with the inclusion of a third component. The three-component fit to the 591 nm kinetics trace is shown in the right panel of **Figure S9.3** with the two-component fit reproduced in the left column for comparison. The three component fit results in a much better fit at 591 nm, with no discernable structure present in the residual.

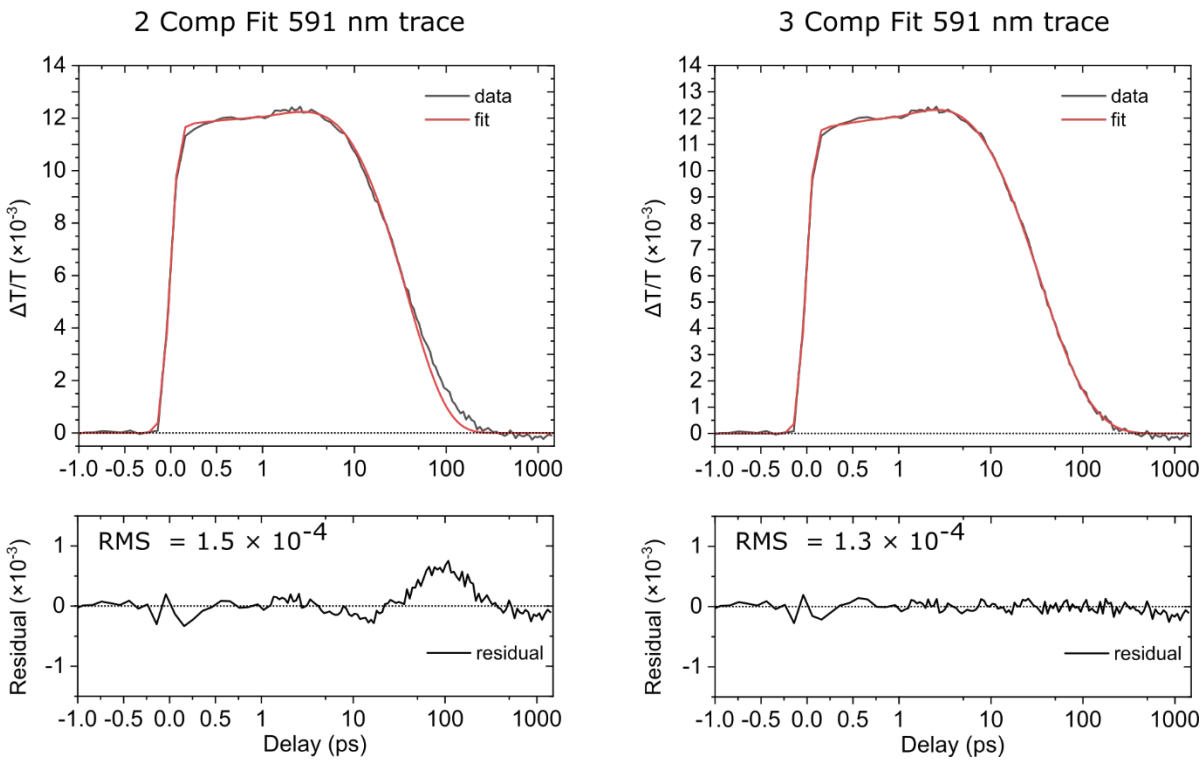

Figure S9.3 Selected kinetics traces (black) and fits (red) taken at 591 nm, which corresponds to a red-shifted shoulder of the ground state bleach of the trimer dimer solution upon 560 nm excitation. (Left) 591 nm kinetics trace and two-component fit of the data with the fit residual plotted below. (Right) 591 nm kinetics trace and three-component fit of the data with the residual plotted below.

While three kinetic components capture the decay at the primary bleach at 591 nm, the fit quality at longer probe wavelengths exhibited notable structure. **Figure S9.4** shows the kinetic trace at 660 nm. The left panel shows the three component fit to the trace. The fit is reasonably good at delays < 100 ps. The residual structure beyond 100 ps delays indicates a long-lived component is present. Since the long-lived component is most apparent at 660 nm, which coincides with the main bleach feature of the monomer, we performed GTA with a fourth component and fixed the rate constant of the component to 1/1.3 ns^{-1} which corresponds to the monomer decay rate. The four-component fit to the 660 nm kinetics trace is shown in the right panel of **Figure S9.4**. The addition of the fourth kinetic component fixed to the monomer lifetime substantially improves the fit at delays greater than 100 ps. Thus, four kinetic components are mathematically justified to fit the TA of the trimer excited at 560 nm.

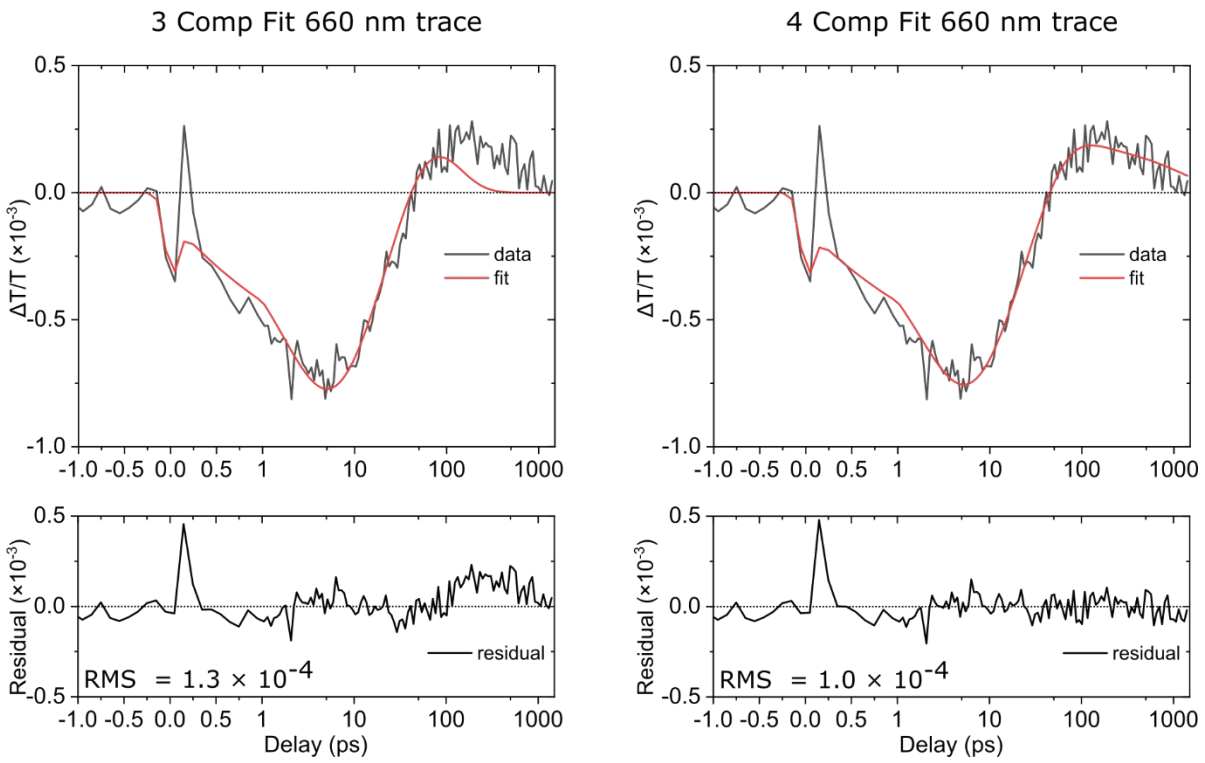

Figure S9.4 Selected kinetics traces (black) and fits (red) taken at 660 nm which overlaps with the primary ground state bleach of the Cy5 monomer. (Left) 660 nm kinetics trace and three-component fit of the data with the fit residual plotted below. (Right) 660 nm kinetics trace and four-component fit of the data with the residual plotted below.

Having demonstrated that the TA of the trimer solution requires four components to achieve a good fit, we now discuss and assign the different components and decay pathways shown in the kinetic scheme in **Figure S9.1**. First, as we argued in **Section S7**, we assign the fourth component to a subpopulation of monomers, and fix its decay rate $k_4 \sim 1/1.3$ ns^{-1}. In the region of the monomer bleach, SAS_4 (**Figure S9.5**, green trace) resembles the monomer.

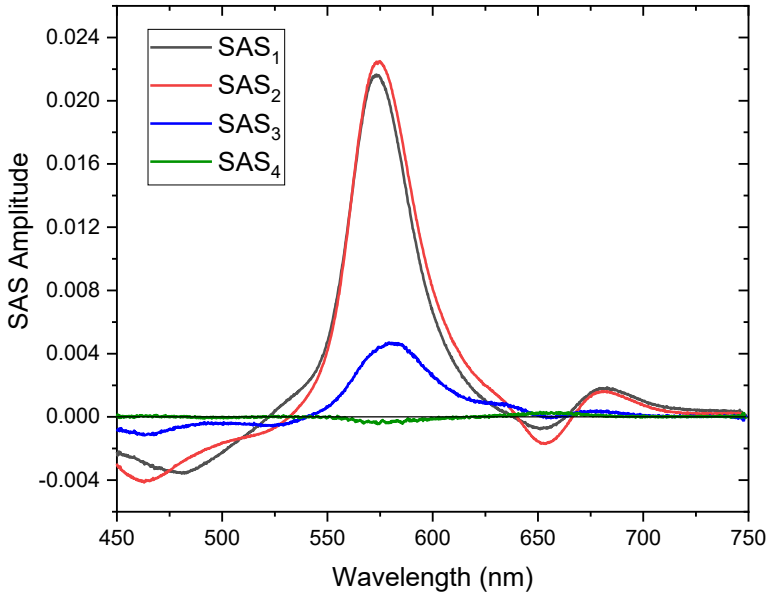

Figure S9.5 Species-associated spectra resulting from a global target analysis of the TA of the type 2 trimer solution according to the four-component kinetic scheme shown in **Figure S9.1**. SAS_1, and SAS_2, are assigned to two components associated with a short-lived trimer sub-population, with the two components decaying in sequence. SAS_3 is assigned to a longer-lived trimer subpopulation decaying in parallel. SAS_4 is assigned to a small subpopulation of monomers also decaying in parallel.

Next, we discuss the first three components, i.e., SAS_1, SAS_2, and SAS_3, and their associated decay rate constants, i.e., k_1, k_2, and k_3. In a previous section (see **S7**), we concluded for the adjacent dimer that the first two kinetic components not belonging to the monomer subpopulation decay in sequence while the third component represented an additional sub-population and was accordingly assigned to decay in parallel. For the trimer, the same relationship between the components is assumed for the following reasons: (i)The trimer dataset, like the adjacent dimer, was also shown by pump wavelength dependent TA to exhibit significant heterogeneity (See **S11** and **S12**), which rules out an exclusively sequential decay scheme for k_1-k_3 (ii) schemes which place k_1 in parallel to the other components result in nonphysical appearing species associated spectra. We are therefore left with the kinetic scheme in which k_1 decays sequentially into k_2, with k_3 and k_4 decaying in parallel.

According to the assignments listed above, the four-component kinetic shown in **Figure S9.1** was determined to be the most appropriate model. The corresponding SAS, shown in **Figure S9.5**, are assigned as a subpopulation of short-lived trimers that undergo sequential kinetics (i.e., SAS_1 and SAS_2), a subpopulation of long-lived trimers (i.e., SAS_3) that decays in parallel, and a small sub-population of monomers (i.e., SAS_4) that also decay in parallel. Importantly, we derived the excited-state decay kinetics of the short-lived and long-lived trimer subpopulations (i.e., k_2 and k_3), which we determine to be ~1/26 and 1/82 ps^{-1}, respectively.

Section S10: Pump wavelength dependence of trimer solution indicates aggregate structural heterogeneity

In order to evaluate whether the type 2 trimer solution exhibited heterogeneity, pump-wavelength depentent transient absorption (TA) measurements were performed. Specifically, TA measurements were conducted with pump wavelengths of 560 and 660 nm (**Figure S10.1**). When the trimer solution is pumped at 560 nm, we observe a single prominent ground-state bleach (GSB) feature centered at ca. 574 nm (**Figure S10.1**, panel A). However, when the trimer solution is pumped at 660 nm, we observe two prominent GSB features centered at ca. 595 and 668 nm (**Figure S10.1**, panel B). Critically, the prominent GSB feature at 574 nm that is observed when pumping the trimer solution at 560 nm is not clearly resolved when pumping the trimer solution at 660 nm; rather, two different GSB features peaking at 595 and 668 nm are observed. These pump-wavelength dependent differences in the GSB features indicate that multiple subpopulations with different absorption spectra are present in the trimer solution. Based on these results, we conclude that the trimer solution exhibits considerable heterogeneity.

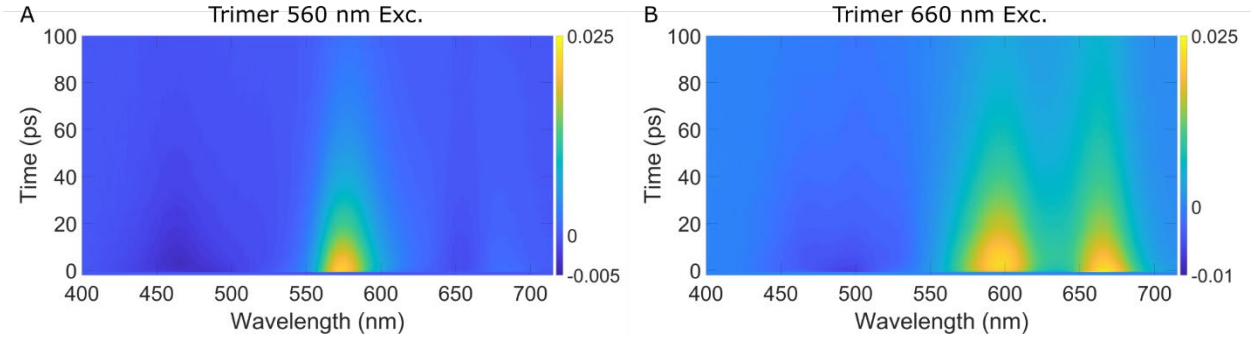

Figure S10.1 Transient absorption of the type 2 trimer solution collected with pump wavelengths of (A) 560 and (B) 660 nm.

Section S11: Gaussian analysis of trimer steady-state absorption spectrum consistent with heterogeneity and multiple subpopulations

To potentially provide additional insight on the heterogeneity in the type 2 trimer solution (as identified in **Section S10**), we performed a Gaussian analysis of the steady-state absorption spectrum. **Figure S11.1** shows that the absorption spectrum is well modeled by five Gaussian lineshapes.

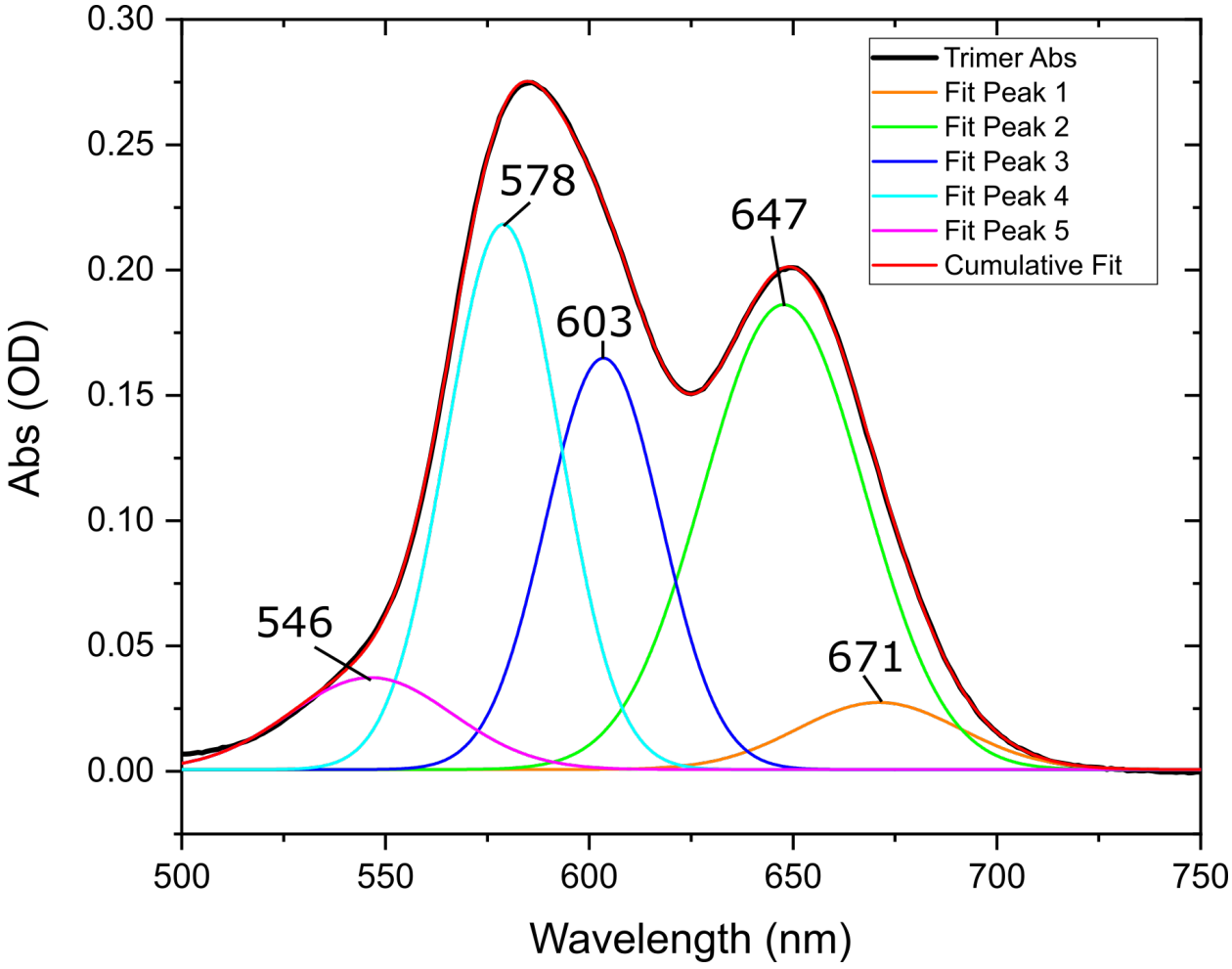

Figure S11.1 Five component Gaussian analysis of trimer absorption spectrum. The trimer absorption spectrum is shown in black, and the cumulative fit is shown in red.

Importantly, the band in the absorption spectrum peaking at ca. 586 nm, which exhibits noticeable asymmetry to its lineshape, is well modeled by two Guassian lineshapes centered at 578 and 603 nm. The 578 nm Gaussian lineshape coincides with the prominent ground-state bleach (GSB) feature at ca. 574 observed for the trimer solution excited at 560 nm. In contrast, the 603 nm Gaussian lineshape better coincides with the strongest GSB feature of the trimer solution excited at 660 nm (see e.g. **Figure S10.1**). Clearly, the results of the Gaussian analysis reinforce the

interpretation in **Section S10**, which indicated that the trimer solution was heterogeneous and likely consists of multiple aggregate subpopulations.

Section S12: Four basis spectrum fit of transient absorption of trimer solution excited at 660 nm

Based on locations of bleach features in trimer TA excited at 660 nm exc **(Fig S10B)** we hypothesized that transverse and adjacent dimer subpopulations exist in the trimer solution. To evaluate this notion, we performed a manual fit of the TA spectrum of the trimer excited at 660 nm and taken at 100 ps delay. Modeling the TA spectrum at 100 ps delay insures that all of the rapid ps and 10s of ps signals that complicate the spectra have largely dissipated. The manual fit was performed by scaling four basis SAS: (i) the SAS corresponding to the excited-state lifetime of the long-lived trimer population (see **Fig. S9.5**, SAS_3), (ii) the SAS corresponding to the transverse dimer excited-state lifetime (see **Fig. S7.5**, SAS3), (iii) the SAS corresponding to the long-lived adjacent dimer (see **Fig. S8.5**, SAS3), and (iv) the SAS of the Cy5 monomer. A wavelength offset was used for the monomer SAS as an additional fitting parameter since the local environment of the monomeric subpopulation in the trimer is likely different than that of the duplex dimer monomer SAS used for the fit. The resulting fit with the scaled basis spectra is shown in **Fig. S.12.1** below.

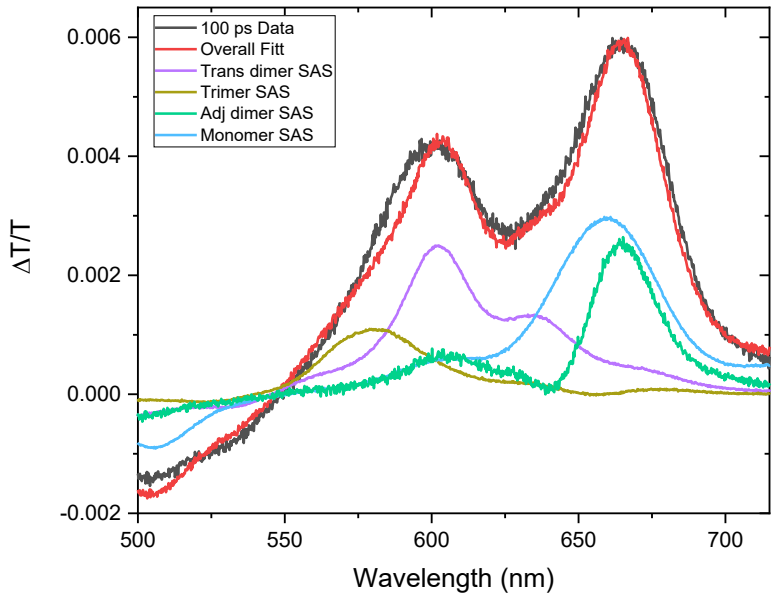

Figure S12.1 The 100 ps delay TA spectra of the trimer solution excited at 660 nm (black), and the manual fit (red) which consists of a sum of the scaled SAS of the long lived trimer (goldenrod), transverse dimer (purple), long-lived adjacent dimer (green), and monomer (blue).

The overall fit is good and suggests that transverse dimer, adjacent dimer, and monomer subpopulations do indeed exist in the trimer solution.

Section S13: Lack of transient absorption pump wavelength dependence indicates type 2 tetramer solution is largely homogeneous

In order to evaluate whether the type 2 tetramer solution exhibited heterogeneity, pump-wavelength dependent transient absorption (TA) measurements were performed. Specifically, TA measurements were conducted with pump wavelengths of 560 and 660 nm (**Figure S13.1**). If the solution were homogeneous, we would expect the two plots to be identical. When the tetramer solution is pumped at 560 nm, a single prominent ground-state bleach (GSB) feature at ca. 565 nm is observed (**Figure S13.1**, panel A). When the tetramer solution is pumped at 660 nm the most intense TA signature is the identical GSB feature at 565 nm (**Figure S13.1** panel B). In addition to the intense GSB feature at 565 nm, a weaker GSB feature is also observed at ca. 660 nm. We attribute this feature to a small subpopulation of monomers based on the following: (i) the GSB feature at 660 nm strongly resembles the most prominent GSB feature in the TA spectrum of the monomer, (ii) the feature persists for the duration of the measurement, i.e., >1 ns, which is consistent with the lifetime of the monomer (**Section S4**), and (iii) the preferential excitation of a small subpopulation of monomers is expected when pumping at 660 nm where the contrast between the absorption strength of the monomer and tetramer is considerable (that is, the monomer absorbance is strong and the tetramer absorbance is weak in this spectral region). Based on these results, we conclude that the type 2 tetramer solution is largely homogeneous, with the exception of a small subpopulation of monomers.

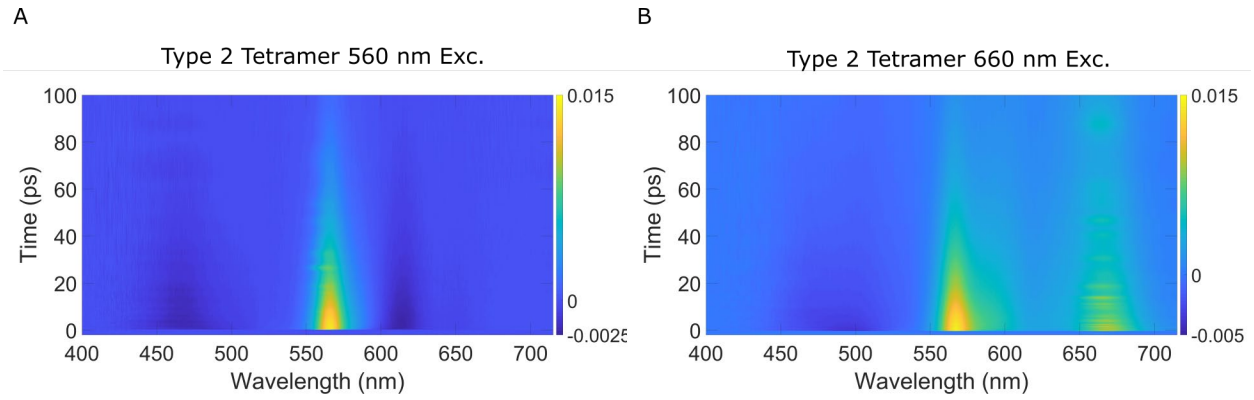

Figure S13.1 Transient absorption of the type 2 Tetramer solution collected with pump wavelengths of (A) 560 nm and (B) 660 nm.

Section S14: Two-component global target analysis of transient absorption of type 2 tetramer solution excited at 560 nm

The spectrotemporal transient absorption (TA) dataset collected for the type 2 tetramer solution excited at 560 nm was subject to global target analysis according to a two-component kinetic scheme shown in **Figure S14.1**. In this supporting section, we discuss the physical and mathematical basis for the two components used to model the TA dataset.

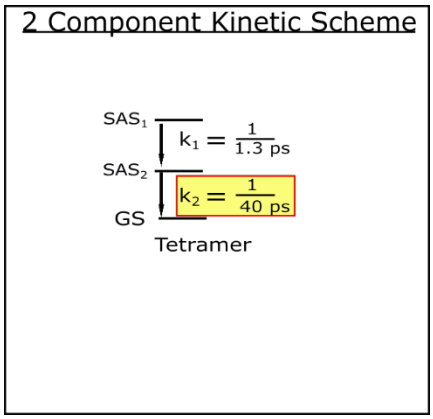

Figure S14.1 The two-component kinetic scheme used in the global target analysis of the transient absorption of the type 2 tetramer solution excited at 560 nm. Both components correspond to a single subpopulation in the solution, the type 2 tetramer structure.

The data were initially globally analyzed using the simplest model including a single component. A reasonably good fit was achieved for the single component fit at the primary bleach feature at 565 nm, as is shown in **Figure S14.2**.

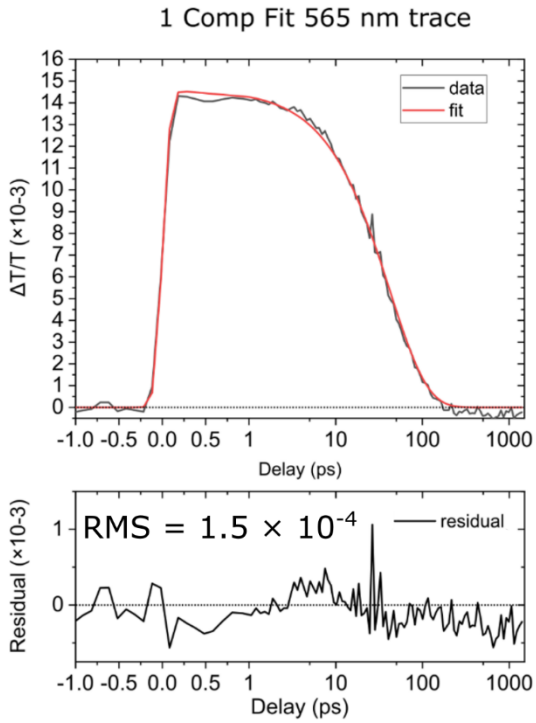

Figure S14.2 Selected kinetics trace (black) and one-component fit (red) taken at 565 nm which corresponds to the primary ground state bleach of the type 2 tetramer solution. The residual is plotted in black below.

While a single kinetic component fit the primary bleach quite well, the fit at the excited state absorption at ca. 470 nm was not as good, with the residual exhibiting structure at delays less < 1 ps (see **Figure S14.3**, left panel). Upon performing the analysis with a second component included, the fit at 470 nm was improved, with no discernable structure in the residual (see **Figure S14.3**, right panel). We therefore conclude that two components are necessary to model these data.

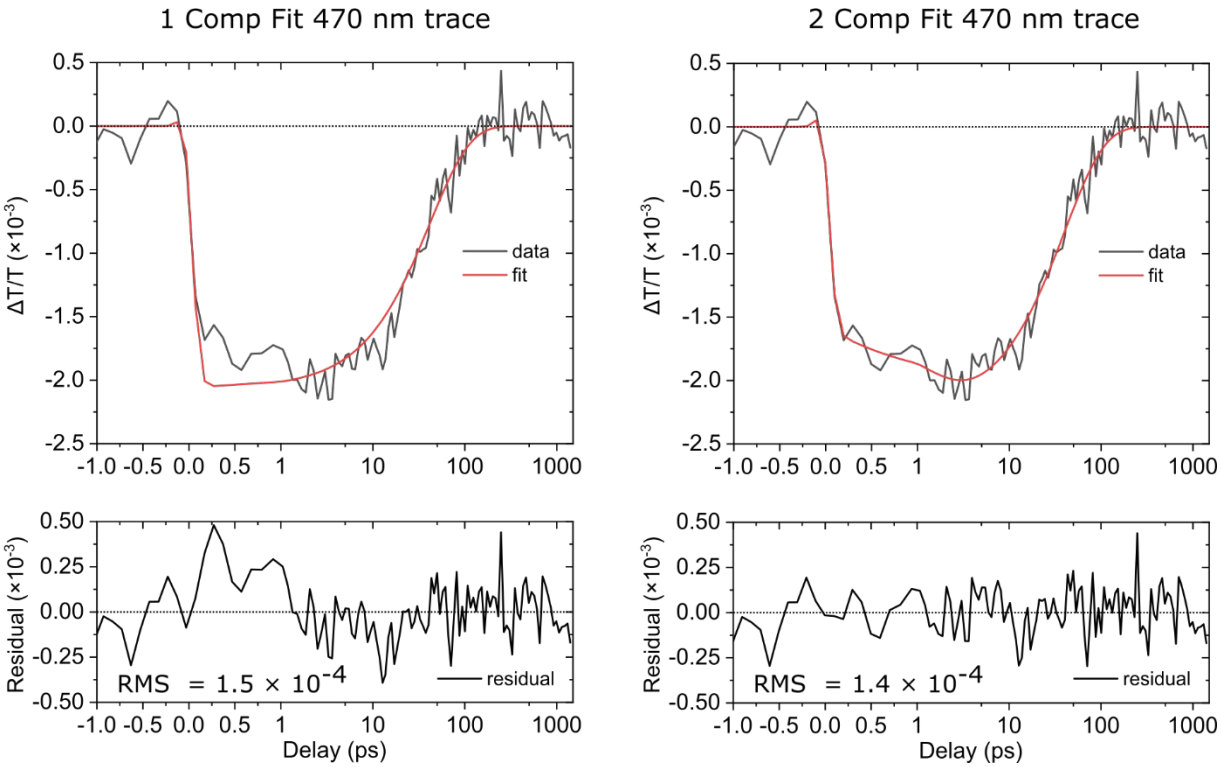

Figure S14.3 Selected kinetics traces (black) and fits (red) taken at 470 nm which corresponds to a prominent ESA of the type 2 tetramer solution. (Left) 470 nm kinetics trace and one-component fit of the data with the fit residual plotted below. (Right) 470 nm kinetics trace and three-component fit of the data with the residual plotted below.

Having demonstrated that two components are needed to fit the TA of the type 2 tetramer solution, we now discuss and assign the different components and decay pathways shown in the kinetic scheme in **Figure S14.1**. Since there are only two components, we must only consider whether they decay in parallel or in sequence. As was discussed for the high-salt type 1 solution excited at 555 nm (**Section S.5**), the parallel decay scenario does not result in SAS with physical characteristics. We therefore conclude that the sequential decaying kinetic scheme shown in **Figure S14.1** is justified. Critically, we are able to derive the excited-state decay kinetics of the type 2 tetramer to be ~1/40 ps^{-1}.

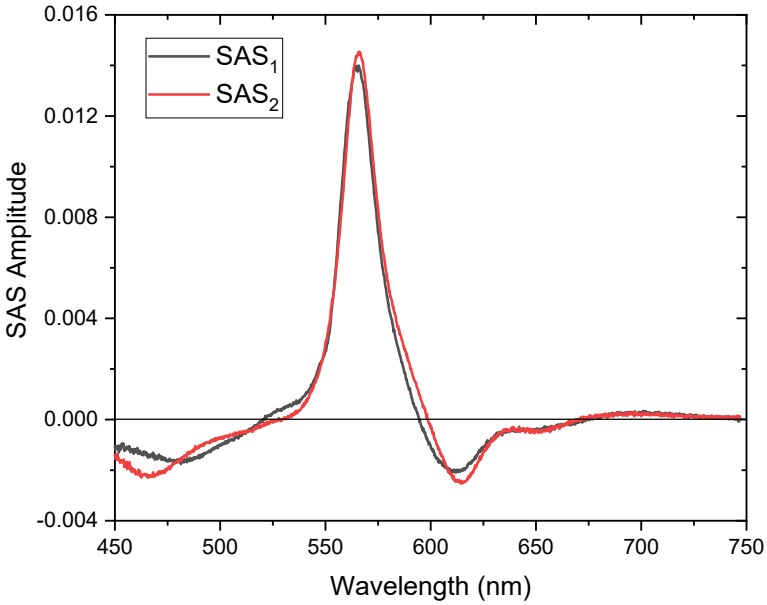

Figure S14.4 Species-associated spectra resulting from a global target analysis of the TA of the type 2 tetramer solution excited at 560 nm according to the two-component sequential kinetic scheme shown in **Figure S14.1**. SAS_1 and SAS_2, are assigned to the sequential decay of the tetramer population.

Section S15: KRM analysis of duplex dimer, transverse dimer, and type 2 tetramer optical properties derives dye packing and excitonic hopping parameter

The packing configurations of the duplex dimer, transverse dimer, and type 2 tetramer were modeled using the most recent version of the in-house software known as the KRM Model Simulation Tool (version 13.7). This was necessary for the duplex dimer because, while the structure has been modeled previously, the newer version of the code, by extracting the transition dipole moment (TDM) directly from the monomer absorbance spectrum, has one fewer fitting parameters. For the transverse dimer and type 2 tetramer, modelling with the most recent version of the KRM code facilitates direct comparison of the derived structures.

Here, we summarize the procedure for modeling aggregate structures, which is described in detail elsewhere.[2,4] Through an initial fitting of the monomer absorption spectrum (**Figure S15.1**, **A**,**C**) a number of parameters are extracted, including the static dipole moment and characteristic exciton hopping parameter of the monomer. The Cy5 monomer exhibits no circular dichroism (CD) as is shown in panels B and D of **Figure S15.1.** Therefore, an initial fit of the CD spectrum is not necessary. To model the aggregate structure, the KRM code accepts several input parameters which include the parameters derived from the initial monomer fit and an initial configuration of the dyes comprising the aggregate. The fitting procedure proceeds by calculating the electronic structure of an aggregate for a range orientations and separations. At each step of the modeling process, the dye configuration is perturbed randomly and the computed extinction and CD spectra for that orientation are compared with the measured extinction and CD spectra for the aggregate. The dye configuration that produces the best simultaneous fit to the extinction and CD spectra is taken to be the best model of the aggregate.

The parameters associated with the best fits of the duplex dimer, transverse dimer, and type 2 tetramer are summarized in **Tables S15.1-S15.3**, respectively. **Tables S15.1-S15.3** list the parameters resulting from the initial monomer fit under "Monomer property", while the electronic and structural parameters resulting from the best fit of the aggregate absorption and CD spectra are listed under "Aggregate parameter". The goodness of the fit of the computed aggregate structure is evaluated with several parameters listed under "Fitting parameters". The first of these fitting parameters is the ratio of the ratios of the theoretical and experimental CD and absorption peak heights given as "RR". The normalized overlap integral for the simulated and experimental absorption and circular dichroism spectra are given as "OI_{ABS}" and "OI_{CD}", respectively. A fitting parameter that includes both overlap terms is "OI_{total}", which is one half the sum of OI_{AB} and OI_{CD}. The mean-square deviations of the computed absorbance and CD spectra are listed as "ms_{ABS}" and "ms_{CD}", respectively. The orientations of the computed TDMs projected onto the XY, YZ, and XZ planes are shown for each aggregate in **Figure S15.2**.

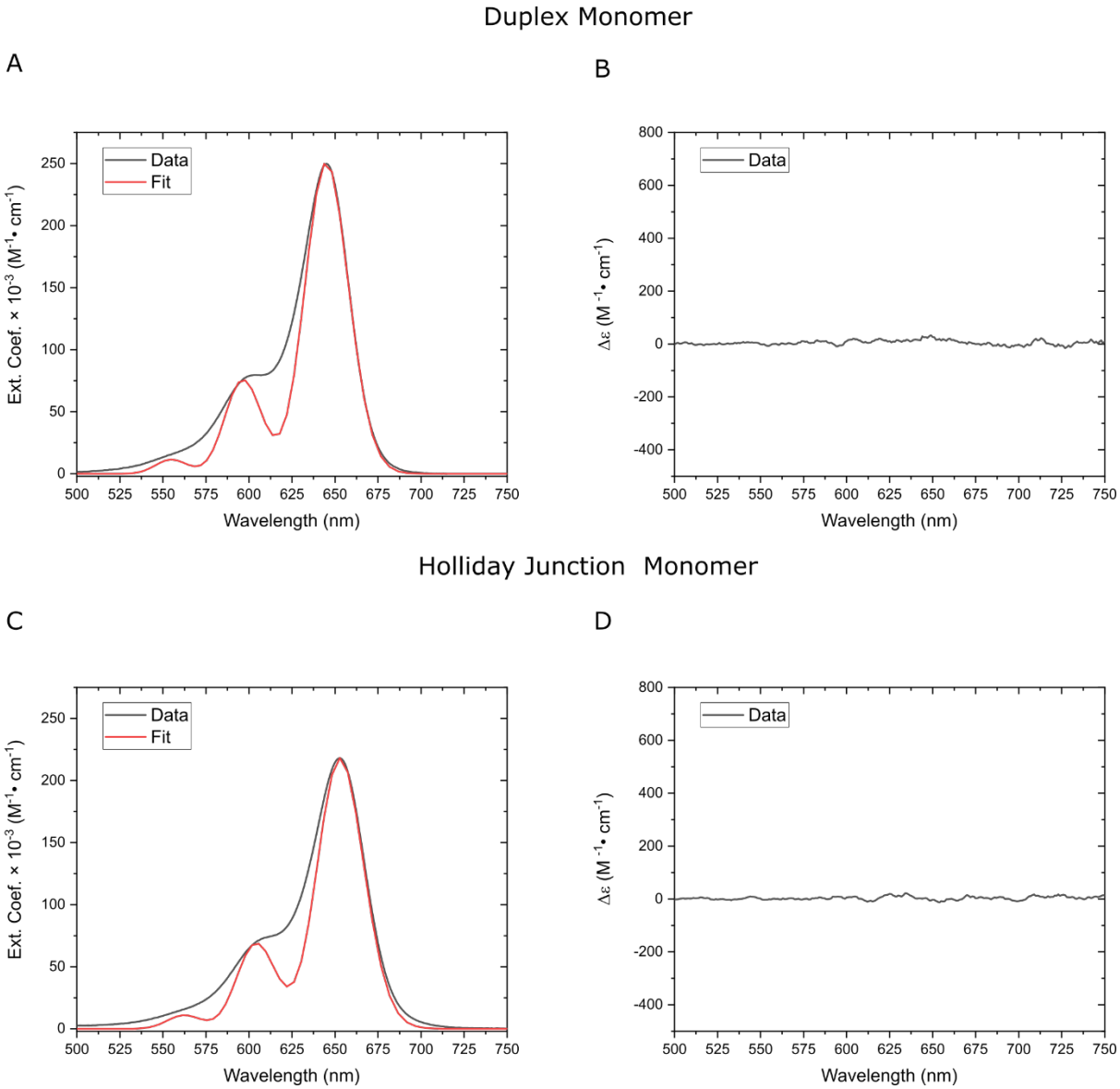

Figure S15.1 (A) Fit (red) of the duplex monomer extinction spectrum (black). (B) The Cy5 monomer attached to duplex DNA shows no circular dichroism in the region of the dye absorption spectrum. (C) Fit (red) of the Holliday junction monomer extinction spectrum (black). (D) The Cy5 monomer attached to the type 2 Holliday junction DNA template shows no circular dichroism in the region of the dye absorption spectrum.

Table S15.1. KRM Parameters associated with the Duplex dimer structure.

Cy5 Duplex Dimer		
Number of chromophores	2	
Number of vibrational levels considered, n_v	3	
Scaffold variant	DNA Duplex	
Monomer propery		**units**
Energy of a vibron ε_v	156	meV
Displacement of excited state potential, *d*, from ground state potential (dimensionless)	0.777	
Energy loss parameter, Γ	37.5	meV
Characteristic excitonic hopping parameter, J_0	62.5	meV*nm^3
Huang-Rhys factor (dimensionless)	0.302	
Transition dipole moment, μ	13.33	debeye
TDM length, *l*	1.4	nm
Energy offset from monomer, *Eof*	-15	meV

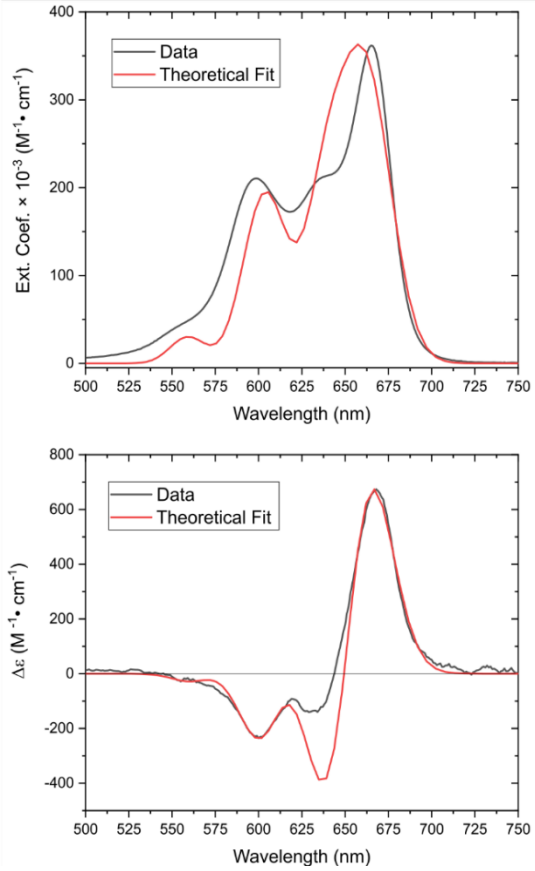

Aggregate parameter	**units**	(1,2)
Exciton hopping parameter, $J_{m,n}$	meV	-48
Center-to-center distance, $R_{m,n}$	nm	1.32
Oblique angle, $\alpha_{m,n}$	degrees	92.7
*Twist angle, $\theta_t^{m,n}$	degrees	-8.9
^Slip angle 1, $\theta_s^{m,R}$	degrees	34.1
^Slip angle 2, $\theta_s^{n,R}$	degrees	58.9

	Center coordinates (nm)			**Angles (degrees)**	
Chromophore number	**X**	**Y**	**Z**	**Zenith**	**Azimuthal**
1	0	0	-0.658	145.9	0
2	0	0	0.658	121.1	-8.9

Fitting parameters	***RR***	***OI$_{ABS}$***	***OI$_{CD}$***	***OI$_{total}$***	***ms$_{ABS}$***	***ms$_{CD}$***
Goodness of fit results	1.02	0.964	0.939	0.951	0.677	0.705

* Twist angle is taken to be the angle between TDM projections in a plane normal to the separation vector, $R_{m,n}$

^ The slip angle depends on the reference dye. Slip angle is the angle between the TDM vector and the separation vector from the reference chromophore

Table S15.2. KRM Parameters associated with the Transverse dimer structure.

Cy5 Transverse Dimer		
Number of chromophores	2	
Number of vibrational levels considered, n_v	3	
Scaffold variant	DNA Holliday Junction	

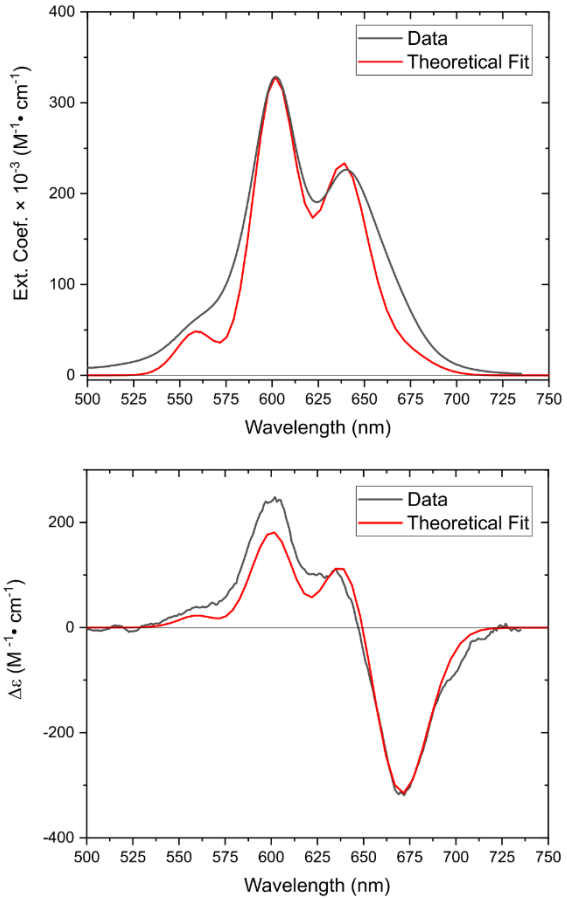

Monomer property		**units**
Energy of a vibron ε_v	153	meV
Displacement of excited state potential, *d*, from ground state potential (dimensionless)	0.795	
Energy loss parameter, Γ	39	meV
Characteristic excitonic hopping parameter, J_0	61.6	meV*nm^3
Huang-Rhys factor (dimensionless)	0.316	
Transition dipole moment, μ	13.24	debeye
TDM length, *l*	1.4	nm
Energy offset from monomer, *Eof*	13	meV

Aggregate parameter	**units**	(1,2)
Exciton hopping parameter, $J_{m,n}$	meV	0.73
Center-to-center distance, $R_{m,n}$	nm	0.68
Oblique angle, $\alpha_{m,n}$	degrees	25.8
*Twist angle, $\theta_t^{m,n}$	degrees	-4.5
^Slip angle 1, $\theta_s^{m,R}$	degrees	68.7
^Slip angle 2, $\theta_s^{n,R}$	degrees	85.8

	Center coordinates (nm)			**Angles (degrees)**	
Chromophore number	**X**	**Y**	**Z**	**Zenith**	**Azimuthal**
1	0	0	-0.340	68.7	0
2	0	0	0.340	94.2	-4.5

Fitting parameters	***RR***	***OI$_{ABS}$***	***OI$_{CD}$***	***OI$_{total}$***	***ms$_{ABS}$***	***ms$_{CD}$***
Goodness of fit results	0.997	0.984	0.977	0.980	0.378	0.493

* Twist angle is taken to be the angle between TDM projections in a plane normal to the separation vector, $R_{m,n}$

^ The slip angle depends on the reference dye. Slip angle is the angle between the TDM vector and the separation vector from the reference chromophore

Table S15.3. KRM Parameters associated with the type 2 tetramer structure.

Cy5 Type 2 Tetramer		
Number of chromophores	4	
Number of vibrational levels considered, n_v	3	
Scaffold variant	DNA Holliday Junction	

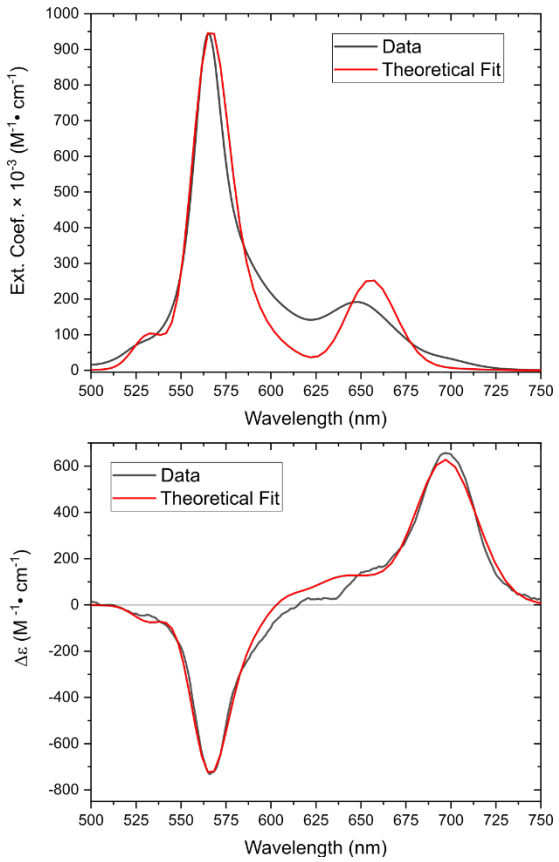

Monomer property		**units**
Energy of a vibron ε_v	153	meV
Displacement of excited state potential, *d*, from ground state potential (dimensionless)	0.795	
Energy loss parameter, Γ	39	meV
Characteristic excitonic hopping parameter, J_0	61.6	meV*nm^3
Huang-Rhys factor (dimensionless)	0.316	
Transition dipole moment, μ	13.24	debeye
TDM length, *l*	1.4	nm
Energy offset from monomer, *Eof*	-11	meV

Aggregate parameter	**units**	(1,2)	(1,3)	(2,3)	(1,4)	(2,4)	(3,4)
Exciton hopping parameter, $J_{m,n}$	meV	12.34	15.80	124.1	15.43	101.9	135.5
Center-to-center distance, $R_{m,n}$	nm	0.996	1.062	0.368	1.154	0.425	0.342
Oblique angle, $\alpha_{m,n}$	degrees	2.7	7.6	5.8	5.1	6.0	6.4
*Twist angle, $\theta_t^{m,n}$	degrees	-2.5	4.8	6.1	5.4	6.6	6.4
^Slip angle 1, $\theta_s^{m,R}$	degrees	38.1	52.5	70.4	59.3	65	85.6
^Slip angle 2, $\theta_s^{n,R}$	degrees	35.9	45.9	71.2	57.2	64.8	85.4

	Center coordinates (nm)			**Angles (degrees)**	
Chromophore number	**X**	**Y**	**Z**	**Zenith**	**Azimuthal**
1	0.375	0.596	-0.022	93.810	-1.144
2	-0.404	0.033	0.243	95.940	0.458
3	-0.245	-0.032	0.568	95.530	6.297
4	-0.206	-0.316	0.381	90.377	2.579

Fitting parameters	***RR***	***OI$_{ABS}$***	***OI$_{CD}$***	***OI$_{total}$***	***ms$_{ABS}$***	***ms$_{CD}$***
Goodness of fit results	0.994	0.9828	0.9927	0.9878	0.2214	0.1563

* Twist angle is taken to be the angle between TDM projections in a plane normal to the separation vector, $R_{m,n}$

^ The slip angle depends on the reference dye. Slip angle is the angle between the TDM vector and the separation vector from the reference chromophore

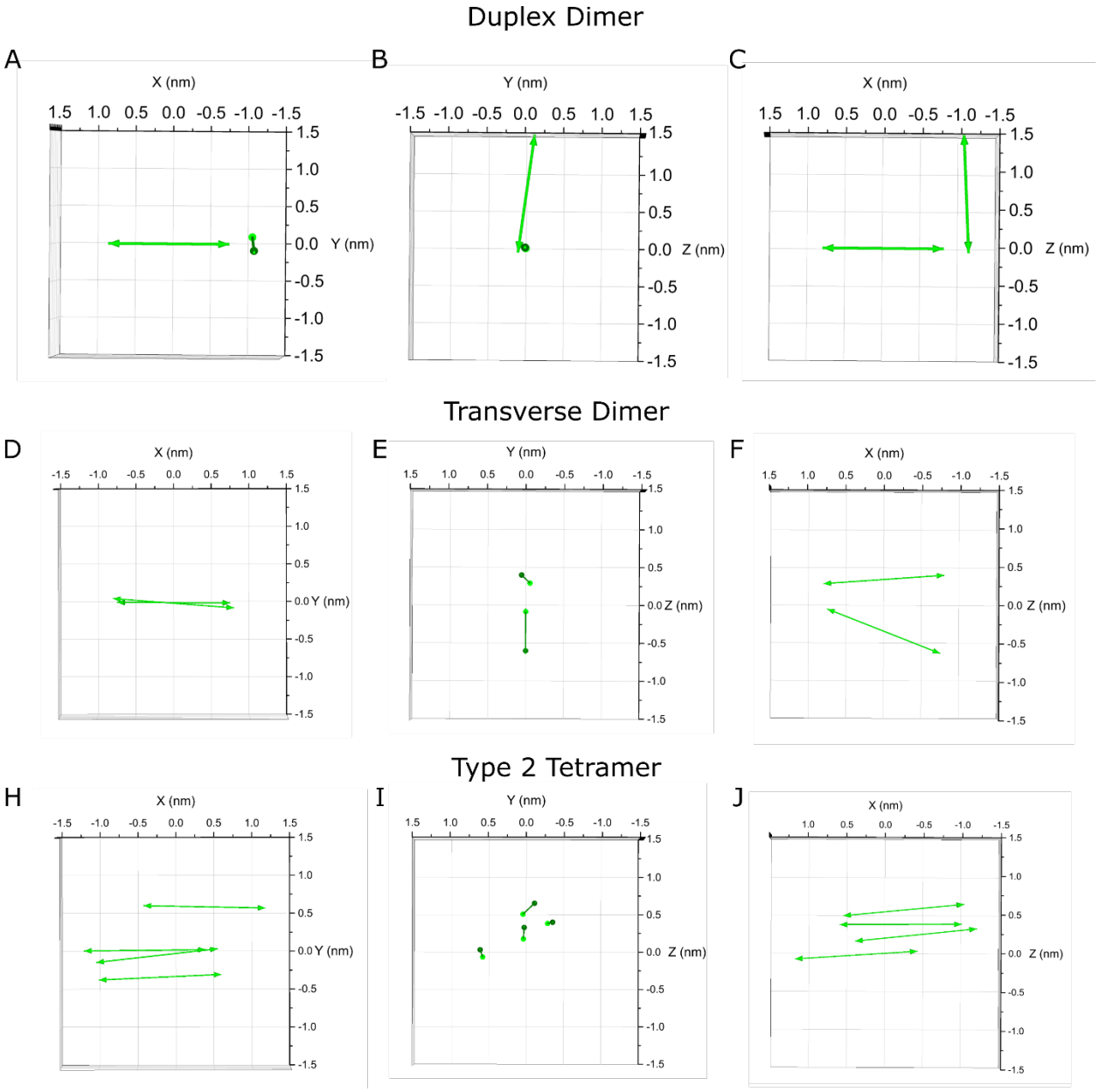

Figure S15.1 Projections along the XY, YZ, and XZ planes of the TDM vectors returned from KRM modeling of the absorption and CD spectra of the duplex dimer (A-C), the transverse dimer (D-F), and the type 2 tetramer (H-J). The TDMs are shown as green double headed arrows.

Section S16: DNA melting curves confirm that Holliday junctions adopt a stacked configuration

The melting temperatures, T_m, were measured for each of the type 2 structures including a monomer and an unlabeled Holliday junction. The solutions were first equilibrated to 25 °C and then ramped to 95 °C at a rate of 1 °C/ min while monitoring the absorption at 260 nm. The resulting melting curves are shown as the main panels in **Figure S16.1**. For each structure, T_m was determined as the midpoint of the logistic function fit to the data.

The logistic function used to fit the data is shown below:

$$f(x) = \frac{L}{1 + e^{-k(x-x_0)}}$$

where L is the maximum, x_0 is the midpoint where the value of $f(x)$ is half the maximum value, and k is the curve steepness.

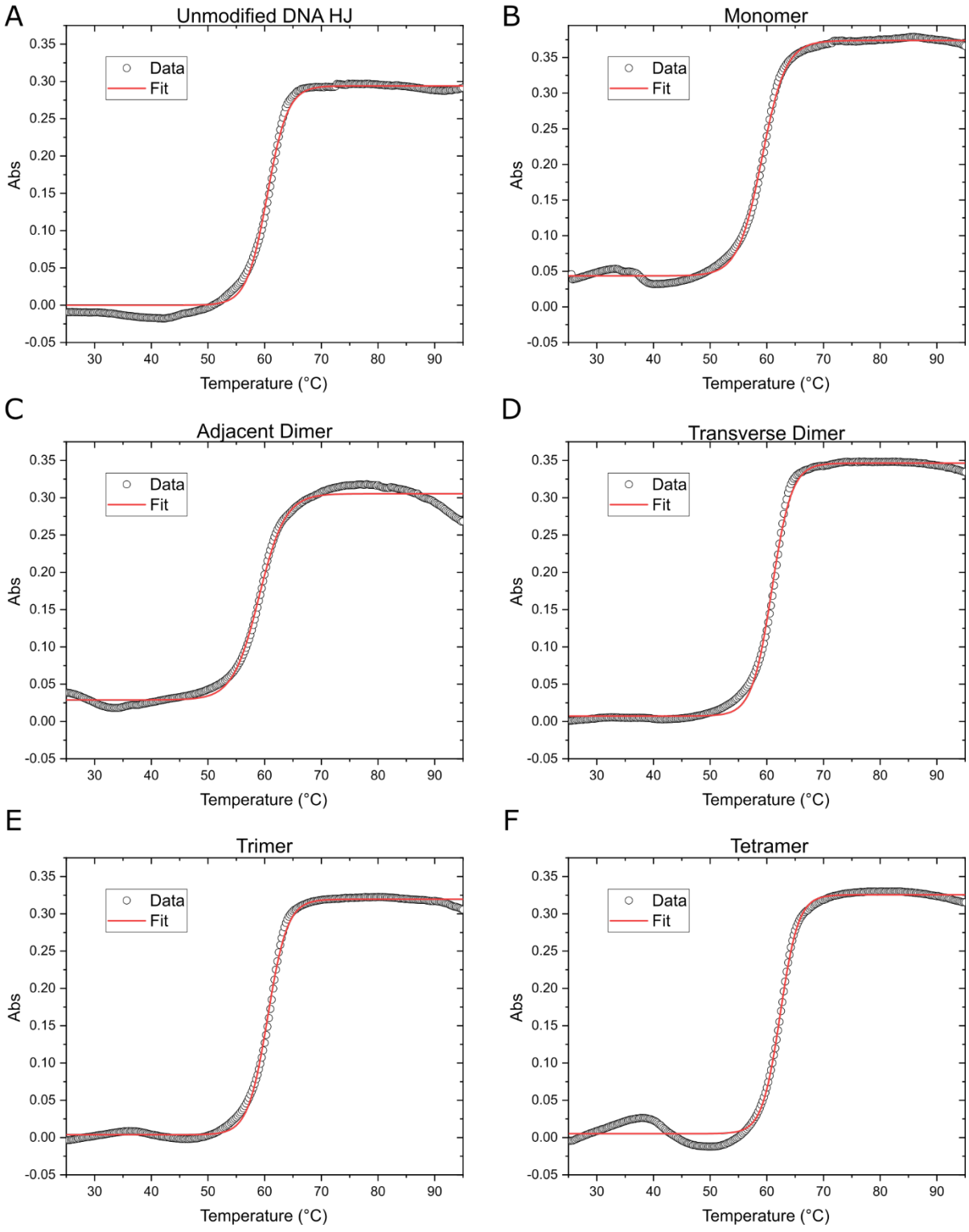
A
Unmodified DNA HJ
B
Monomer
C
Adjacent Dimer
D
Transverse Dimer
E
Trimer
F
Tetramer
Data
Fit
Abs
Temperature (°C)

Figure S16.1 Melting profiles (circles) and logistic function fits (red lines) of the (A) unmodified Holliday junction, (B) Holliday junction with a Cy5 label at the D position, (C) adjacent dimer, (D) transverse dimer, (E) trimer, and (F) Tetramer solutions in 1 × TAE 15 mM $MgCl_2$.

Supplementary Table S16.1 Melting temperatures of several Holliday junction structures.

Construct[a]	**T_m (°C)**
Unmodified DNA HJ, 100 mM NaCl	48.5
Unmodified DNA HJ, 15 mM MgCl	60.5
Monomer D	59.1
Adjacent dimer	59.0
Transverse dimer	60.9
Trimer	60.5
Tetramer	62.4

[a] Buffer conditions for all solutions are 1 × TAE. For the unmodified construct solutions, the added salt concentrations are indicated. For the dye labeled construct solutions, the added salt concentration is 15 mM $MgCl_2$.

Mass *et al.* previously reported melting temperatures of 60.0 and 46.7 °C for the same unmodified DNA Holliday junction studied here in 15 mM $MgCl_2$ and 100 mM NaCl solution conditions, respectively. From these results they determined that $MgCl_2$ causes the Holliday junction to take on a stacked configuration, while NaCl promotes an open configuration.[5] We measured the melting temperatures of the unlabeled Holliday junction to be 60.5 and 48.5 °C in 1 × TAE for 15 mM $MgCl_2$ and 1 × TAE 100 mM NaCl buffer conditions, respectively, which are similar to the values reported by Mass *et al.* The melting curve of the unmodified DNA HJ in 100 mM NaCl buffer conditions is shown in **Figure S.16.2**. We therefore conclude that, based on the similarity of the measured melting temperatures of the dye labeled Holliday junctions to the unlabeled Holliday junction in 1 × TAE 15 mM $MgCl_2$, the Holliday junctions in all of the dye labeled type 2 solutions adopt a stacked configuration.

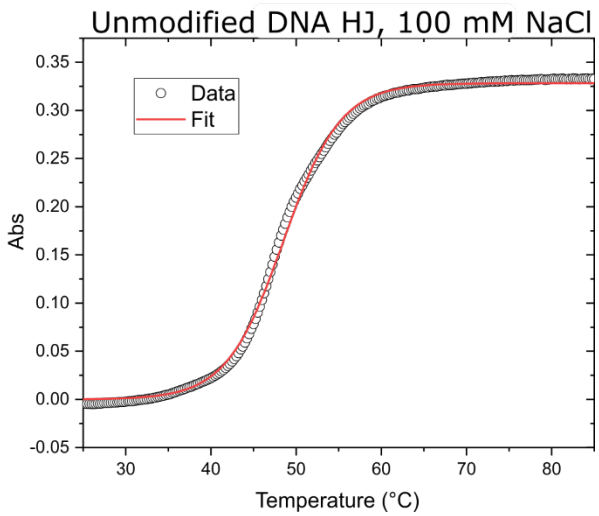

Figure S16.2 Melting profile and logistic function fit of the unmodified DNA Holliday junction at 1 × TAE 100 mM NaCl buffer conditions.

Section S17: Holliday junction stacked isomers differ by the co-facially stacked bases

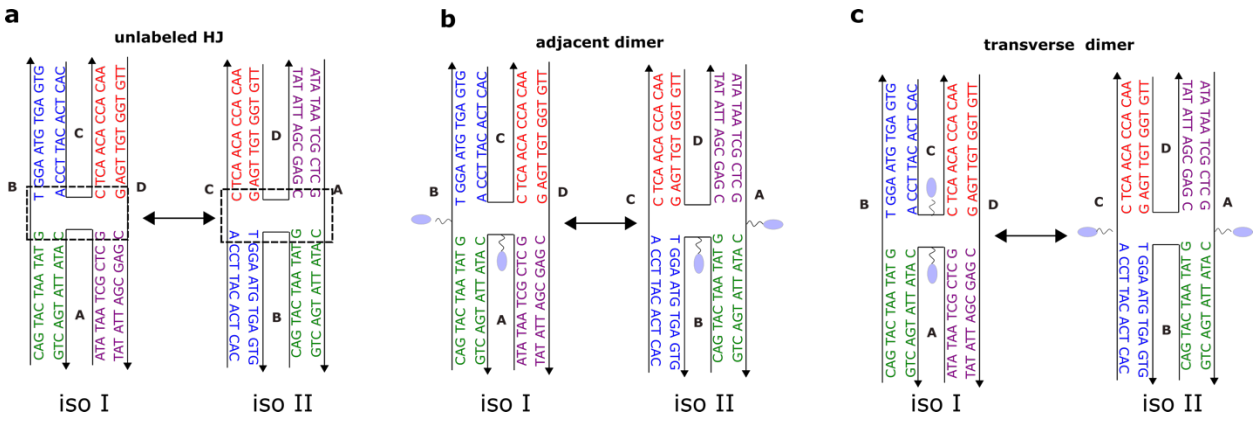

Fig. S17.1 The two iso I and II stacked DNA Holliday junction configurations present in the DNA and DNA-dye construct solutions with 15 mM $MgCl_2$ added. Schematic representations of the iso I and II configurations present in the **(a)** unlabeled Holliday junction solution, **(b)** adjacent dimer solution, and **(c)** transverse dimer solution. The dashed squares in panel **a** highlight four base pairs co-facially stacked in each isomer of the unlabeled Holliday junction. In panels **b** and **c**, blue ovals indicate positions of dye labels.

Section S18: Type 2 Holliday junctions may exhibit “semi-mobility”

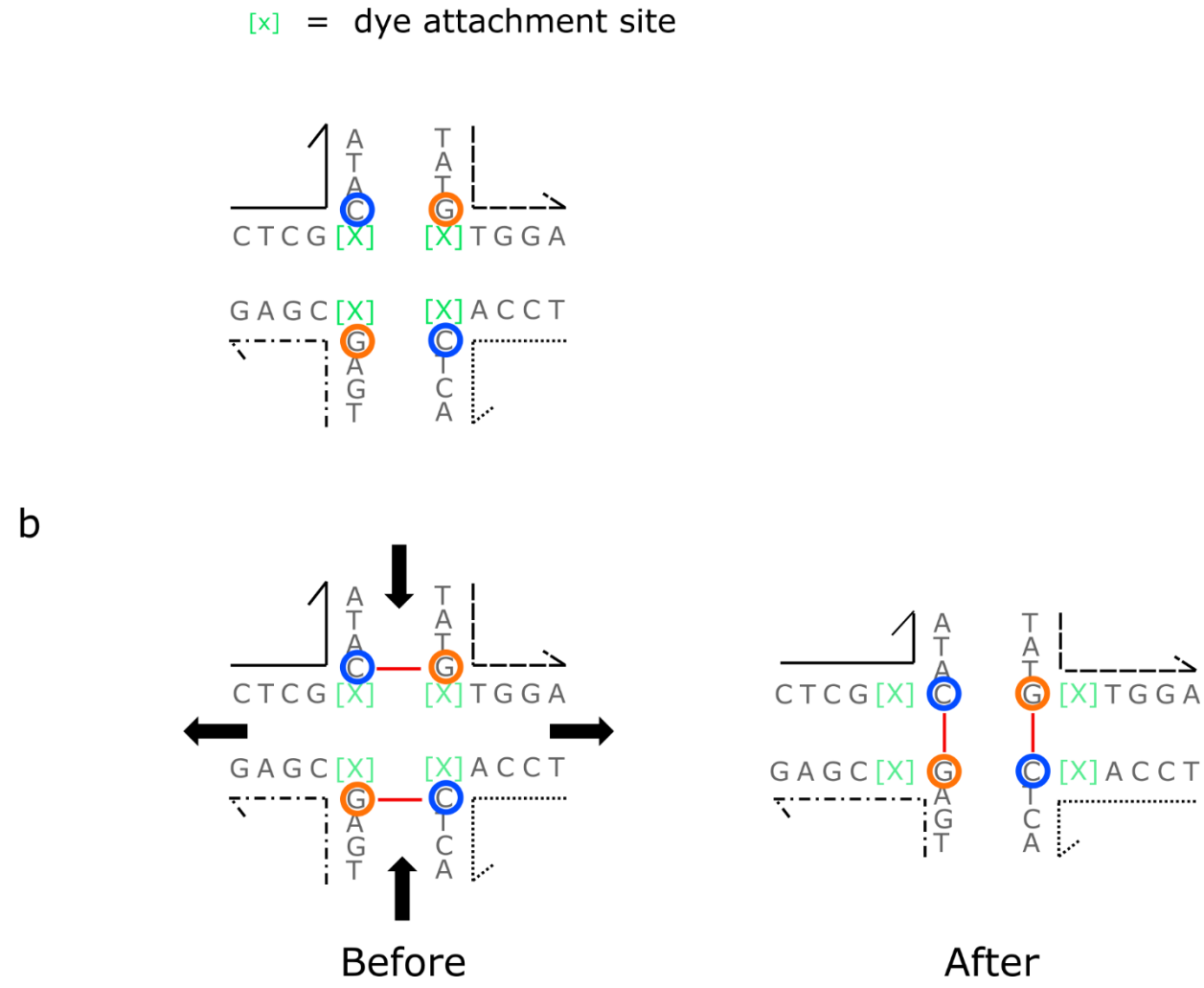

Figure S.18.1 Schematic illustration of semi-mobility in the type 2 Holliday junction. (a) Cropped view showing the inner 8 bases of the type 2 Holliday junction. The arms of the Holliday junction are the same length for this configuration. The complementary cytosine and guanine bases responsible for semi-mobility are circled in blue and orange, respectively, and the dye attachment sites are shown in green. (b) The two type 2 Holliday junction configurations accessible through semi-mobility. The left schematic shows the structure with all arms of equal length, while the right shows the same junction after the vertical and horizontal arms have exchanged a base. Red lines illustrate which of the cirlced bases are paired for each configuration.

Section S19: Supplemental methods

Pump Autocorrelation via Polarization Gating. The pulse duration of the optical parametric amplifier (OPA) was measured at 650 nm using polarization gating.[6] The OPA output was split, and one beam was directed into the pump arm of the TA spectrometer while the other beam was directed into the probe arm. The pump and probe relative polarizations were set to 45 degrees and a polarizer was placed after sample position and set to null the probe. The pump and probe were overlapped within a 2 mm quartz cuvette filled with distilled water. When the pump and probe overlapped spatially and temporally within the cuvette, the probe polarization was slightly rotated due to the optical Kerr effect, allowing some of the probe to transmit through the polarizer and into the detector. The pump and probe delay was then scanned to collect an autocorrelation.

Time Correlated Single Photon Counting. The Cy5 Holliday junction monomer fluorescence lifetime was measured using a PicoQuant Fluorolog 250 (PicoQuant, Berlin) time correlated single photon counting (TCSPC) instrument. The monomer solution was excited with a 650 nm 32MHz pulsed diode laser. The fluorescence emission passed through a polarizer set to the magic angle with respect to the excitation and was detected at 680 nm.

For the measurement, a dilute solution of the monomer labeled Holliday junctions was prepared by diluting a portion of the concentrated monomer solution prepared for transient absorption such that the optical density was approximately 0.05 at the Cy5 absorption maximum of 655 nm. The solution was stirred in a 1 cm quartz cuvette (Starna Cells, Inc.; Atascadero, CA, USA).

Circular Dichroism Spectroscopy. A Jasco J-1500 spectropolarimeter (JASCO, Easton, MD) was used to collect the circular dichroism (CD) spectra used in the KRM analysis. CD spectra were collected for solutions of the duplex and Holliday junction Cy5 monomer, the duplex dimer, the transverse dimer, and the type 2 tetramer. The CD signal was measured from 200 to 800 nm at a rate of 200 nm/min in 1 nm steps. A 1 cm path length quartz micro cuvette (JASCO 0553, 100 μL capacity) was used.

Melting Curve measurement. A Cary5000 spectrophotometer equipped with a thermal probe (Agilent Technologies Cary Temperature Controller G9808) was used to measure the denaturation temperatures of the DNA-Cy5 constructs. Samples were first degassed for 5 minutes at room temperature then equilibrated at 25 °C for 2 minutes. The temperature was ramped at 1 °C/min from 25 °C to 95 °C while monitoring the absorption at 260 nm.

Section S20: Supplemental references

(1) Huff, J. S.; Davis, P. H.; Christy, A.; Kellis, D. L.; Kandadai, N.; Toa, Z. S. D.; Scholes, G. D.; Yurke, B.; Knowlton, W. B.; Pensack, R. D. DNA-Templated Aggregates of Strongly Coupled Cyanine Dyes: Nonradiative Decay Governs Exciton Lifetimes. *J. Phys. Chem. Lett.* **2019**, *10*, 2386–2392.

(2) Cannon, B. L.; Kellis, D. L.; Patten, L. K.; Davis, P. H.; Lee, J.; Graugnard, E.; Yurke, B.; Knowlton, W. B. Coherent Exciton Delocalization in a Two-State DNA-Templated Dye Aggregate System. *J. Phys. Chem. A* **2017,** *121*, 6905-6916.

(3) Barclay, M. S.; Roy, S. K.; Huff, J. S.; Mass, O. A.; Turner, D. B. Rotaxane Rings Promote Oblique Packing and Extended Lifetimes in DNA-Templated Molecular Dye Aggregates. *Commun. Chem.* **2021**, *4,* 19.

(4) Cannon, B. L.; Patten, L. K.; Kellis, D. L.; Davis, P. H.; Lee, J.; Graugnard, E.; Yurke, B.; Knowlton, W. B. Large Davydov Splitting and Strong Fluorescence Suppression: An Investigation of Exciton Delocalization in DNA-Templated Holliday Junction Dye Aggregates. *J. Phys. Chem. A* **2018**, *122*, 2086–2095.

(5) Mass, O. A.; Wilson, C. K.; Roy, S. K.; Barclay, M. S.; Patten, L. K.; Terpetschnig, E. A.; Lee, J.; Pensack, R. D.; Yurke, B.; Knowlton, W. B. Exciton Delocalization in Indolenine Squaraine Aggregates Templated by DNA Holliday Junction Scaffolds. *J. Phys. Chem. B* **2020**, *124*, 9636–9647.

(6) Trebino, R.; DeLong, K. W.; Fittinghoff, D. N.; Sweetser, J. N.; Krumbügel, M. A.; Richman, B. A.; Kane, D. J. Measuring Ultrashort Laser Pulses in the Time-Frequency Domain Using Frequency-Resolved Optical Gating. *Rev. Sci. Instrum.* **1997**, *68*, 3277–3295.